UNCLASSIFIED

AD NUMBER
AD849932
NEW LIMITATION CHANGE
TO Approved for public release, distribution unlimited
FROM Distribution authorized to U.S. Gov't. agencies and their contractors; Critical Technology; FEB 1969. Other requests shall be referred to Rome Air Developmental Center, Griffiss AFB, NY 13440.
AUTHORITY
RADC ltr, 17 Sep 1971

THIS PAGE IS UNCLASSIFIED

AD849932

RADC-TR-69-21
Final Technical Report
February 1969

WIDEBAND MAGNETOELASTIC FREQUENCY-SELECTIVE LIMITER FOR VHF

Roger W. Orth

The Boeing Company

This document is subject to special export controls and each transmittal to foreign governments, foreign nationals or representatives thereto may be made only with prior approval of RADC (EMIAD), GAFB, N.Y. 13440.

D D C
APR 1 1969
B

Rome Air Development Center
Air Force Systems Command
Griffiss Air Force Base, New York

When US Government drawings, specifications, or other data are used for any purpose other than a definitely related government procurement operation, the government thereby incurs no responsibility nor any obligation whatsoever, and the fact that the government may have formulated, furnished, or in any way supplied the said drawings, specifications, or other data is not to be regarded, by implication or otherwise, as in any manner licensing the holder or any other person or corporation, or conveying any rights or permission to manufacture, use, or sell any patented invention that may in any way be related thereto.

Do not return this copy. Retain or destroy.

WIDEBAND MAGNETOELASTIC FREQUENCY-SELECTIVE LIMITER FOR VHF

Roger W. Orth

The Boeing Company

This document is subject to special export controls and each transmittal to foreign governments, foreign nationals or representatives thereto may be made only with prior approval of RADC (EMIAD), GAFB, N.Y. 13440.

FOREWORD

This report was completed under Contract F30602-68-C-0072, Project 5573, Task 557301, sponsored by Rome Air Development Center, Griffiss Air Force Base, Rome New York 13440. The Air Force Contract Monitor is H. Friedman, EMIAD. The report summarized 1968 research, stressing work conducted during the period 1 July 1968 through 31 December 1968 by The Boeing Company, Aerospace Systems Division, Seattle, Washington. This report has a Boeing internal Document Number D2-125920-2. The First Technical Report has a Boeing internal Number of D2-125920-1. The program manager is John D. Belenski.

The author wishes to acknowledge the valuable contributions of Drs. Darrell R. Jackson, Attelio Giarola, and Bruce McLeod, and of Charles Strickland, who conducted many of the laboratory evaluations.

This technical report has been reviewed and is approved.

Henry Friedman

Approved: HENRY FRIEDMAN
Task Engineer

Approved: V.E. STOLL, Colonel, USAF
Chief, Intel & Info Processing Division

FOR THE COMMANDER:
IRVING J. GABELMAN
Chief, Advanced Studies Group

ABSTRACT

In this Second Technical Report, the results of one year's progress are summarized for RADC Contract F30602-68-C-0072, titled "Wideband Magnetoelastic Frequency-Selective Limiter for VHF Band," for the construction of a frequency-selective limiter that uses parametric generation of subharmonic magnetoelastic modes in ferrimagnetic materials. Special attention is given to the results of tests performed during the second six months on the broadband models constructed. Based on the theory of operation and test results presented in the First Technical Report, the philosophy of broadband frequency-selective limiter circuit design is presented. The importance of pumping direction, material selection, and orientation is discussed.

The material used in the final model is YIG:Ga, a highly doped garnet. The final orientation was made to provide a low internal saturation magnetic field to provide a low limiting threshold. Tests of the final model indicated that extremely selective limiting (about 3 KHz selectivity), low intermodulation levels, and linear small signal phase response are obtainable at VHF.

TABLE OF CONTENTS

Section	Title	Page
I	INTRODUCTION	1
II	MATERIAL CONSIDERATIONS	9
III	PUMPING DIRECTION	17
IV	CIRCUIT DESIGN	20
V	MAGNET REQUIREMENTS	30
VI	TESTING	31
VII	CONCLUSIONS	62
VIII	RECOMMENDED FOLLOW-ON PROGRAM	65
	REFERENCES	67

LIST OF ILLUSTRATIONS

Figure	Title	Page
1.	Magnetoelastic, Spin and Elastic Waves	4
2.	Basic Magnetoelastic Limiter (Parallel Pumped)	6
3.	Temperature Dependence of Material Parameters	12
4.	Approximate Domain Orientation Versus Applied Bias Field Strength	14
5.	Basic Circuit	22
6.	Cascaded Parallel-Resonant Circuits	24
7.	Seven-Sphere Cascaded Series-Resonant Circuits	25
8.	Basic Lowpass Prototype Filter	27
9.	Intermediate Bandpass Prototype Network	27
10.	Conditioned Bandpass Filter Network	28
11.	Normalized (Equal Inductance) Bandpass Filter	28
12.	Two-Sphere Cascaded Parallel Resonant Circuits	33
13.	Limiting Curve for Transverse Pumping with Three Spheres	35
14.	Limiting Curve for Transverse Pumping with Three Spheres (Wideband)	36
15.	Limiting Curve for Parallel Pumping with Three Spheres	38
16.	Picture of the Three-Sphere Final Breadboard Model	39
17.	Threshold of Cascaded Three Sphere FSL	40
18.	Small Signal Insertion Loss of Cascaded Three Sphere FSL	40
19.	Dynamic Range of Cascaded Three Sphere FSL	41
20.	Phase Shift of Cascaded Three Sphere FSL (In-band Response)	41
21.	Small Signal Amplitude Response of Cascaded Three Sphere FSL	42

Figure	Title	Page
22.	Phase Shift of Cascaded Three Sphere FSL	43
23.	Maximum Intermodulation Component Level	44
24.	Maximum Intermodulation Component Level	45
25.	Selectivity of Cascaded Three Sphere FSL	46
26.	Limiting Curves for Cascaded Three Sphere FSL	47
27.	Block Diagram of System Used to Measure Intermodulation Characteristics	48
28.	Block Diagram of System Used to Measure Small Signal Amplitude Characteristics	49
29.	Block Diagram of System Used to Measure Limiting Characteristics	50
30.	Picture of the Seven Sphere FSL	52
31.	Measured Small Signal Response of the Seven Sphere FSL	53
32.	Phase Response of the Seven Sphere FSL	54
33.	Phase Response of the Seven Sphere FSL (In-Band)	55
34.	Dynamic Limiting Range of the Seven Sphere FSL	56
35.	Dynamic Limiting Range of the Seven Sphere FSL When Adjusted for Good Limiting	57
36.	Limiting Curve for the Seven Sphere FSL	58
37.	Level of Largest Intermodulation Component	59
38.	Intermodulation Levels	60

LIST OF TABLES

Table	Title	Page
1	Characteristics of Normalized Passband Filters	29
2	Comparison of Design Objectives and Measured Characteristics of Field Models	63

SECTION I

INTRODUCTION

Frequency-selective limiters have been developed for operation over various frequency ranges, although not all are beyond the "laboratory model" stage of development. A frequency-selective limiter is a two-port device that can adapt its passband frequency response to selectively attenuate signals on a power-density basis. The frequency-selective limiter (FSL) can be constructed using nuclear magnetic resonance to operate with a center frequency in the range from 10 KHz to 50 MHz. The FSL using parametric subharmonic generation of coincidence spin waves can be constructed for operation above VHF. Subsidiary resonance devices have been operated at S-band and above. The FSL using electron paramagnetic resonance has been operated at X-band and could be extended to operation in the range from P to K-band. The FSL described in this report uses parametric generation of subharmonic magnetoelastic waves and operates in the VHF region, filling a gap in FSL frequency coverage. The principal aim of the work reported here is to broaden the instantaneous bandwidth of the basic magnetoelastic FSL to a value substantially beyond the 1 - 2% figure obtained in earlier experimental models (References 1 and 2), to lower the insertion loss, and increase the limiting dynamic range.

I.1 PROGRAM

The contract work statement required the following effort:

a. Study and Investigation of magnetoleastic limiting phenomena shall be made to obtain wideband frequency-selective limiters in the VHF-Bands. The program shall include study of effective magnetoelastic coupling and DC saturation field with crystal orientation; elastic and spin-wave damping effects; optimization of limiting and bandwidth characteristics; and development of broadbanding techniques using multiple spheres.

b. Breadboarding to determine the feasibility of achieving the following design objectives:

(1) Center frequency	150-250 MHz
(2) Instantaneous 3 dB bandwidth	20% to an octave
(3) Limiting dynamic range	15-30 dB
(4) Average insertion loss	3 dB to 0.5 dB
(5) Passband ripple	± 2 dB to ± 0.5 dB
(6) Limiting threshold	0 to -20 dBm

c. Test and Evaluation of breadboarded limiters to determine the extent to which the performance objectives specified in paragraph b. above have been achieved. The evaluation shall include determination of small signal amplitude and phase response over the frequency range 50-400 MHz. Linearity, intermodulation effects, and frequency-selective limiting performance shall be determined as a function of input power level and operating frequency.

The work of paragraph a. above was completed during the first six months, and was discussed in the First Technical Report dated July 1968. A summary of that work appears in Section 1.3 below. The work defined in paragraphs b. and c. was completed during the second six months and will be discussed in this report.

I.2 CONCEPTS OF OPERATION

The FSL considered in this contract is a parametric device. Magnetoelastic waves (coupled spin waves of the magnetic system and elastic waves of the elastic system) are parametrically excited at one half the input (pump) frequency. The nonlinearity required for parametric coupling exists between an input resonant circuit and the magnetic system of the ferrimagnetic crystal used, as discussed in the First Technical Report. This allows the losses of the magnetoelastic modes

to be supplied by the input signal through the magnetic spin system. When the losses are (almost) completely supplied at some frequency, 2ω, the amplitude of the subharmonic magnetoelastic mode at half that frequency will increase, and the FSL input reflection coefficient at that frequency will indicate a mismatch. As a result, the output power at 2ω will be limited.

The allowed modes of oscillation for the coupled spin (magnetic) and elastic systems are shown in Figure 1. The (uncoupled) elastic system has modes lying along the straight line ①, $\omega = ck$ where c is the wave velocity, and k is the wave number. The (uncoupled) spin system has modes falling between the dotted lines of Figure 1 where the upper line represents a pure spin wave propagating at 90° with respect to the applied d.c. bias magnetic field $\bar{H}_o$ and the lower dotted line represents a pure spin wave propagating along $\bar{H}_o$. The spin wave frequency is

$$\omega_k = \gamma\sqrt{H_{oo}(H_{oo} + H_a)} \qquad \text{(I-1)}$$

where $H_{oo} = H_o - N_z M_s + Dk^2 + H_{a2}$

$\gamma/2\pi = 2.81(10^6)$ Hz per oersted

$H_a = H_{a1} - H_{a2} + 4\pi M_s \sin^2 \theta_D$

$N_z = 4\pi/3$ for sphere

H_{a1} and H_{a2} are anisotropy field terms dependent on crystal orientation, θ_D is the propagation angle with respect to $\bar{H}_o$, and M_s is the saturation magnetization.

The equation for the dotted curves goes as k^2 at large values of k due to the exchange coupling between spins. In the upper k region, the waves are said to be exchange dominated. The regions ② and ③ are the interaction regions where the waves are designated magnetoelastic. The separation between regions ② and ③ is governed by the amount of interaction and can be used as an estimate of the shift in frequency needed to go from pure elastic modes to pure spin wave modes. Further discussion was presented in the First Technical Report.

Any of the modes shown in Figure 1 may be parametrically excited but the threshold power level at which this occurs differs significantly between regions. The pure spin waves have a much lower threshold than the elastic waves, provided spin wave modes are available at 1/2 the pump frequency. In the region ③, the high propagation angle waves

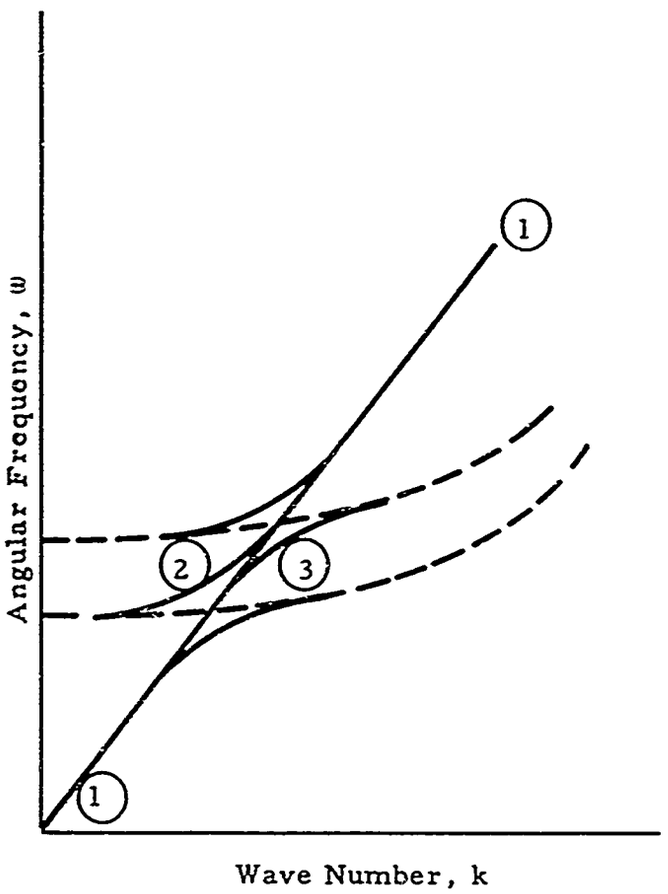

Figure 1 Magnetoelastic, Spin and Elastic Waves

have a lower threshold than those propagating along $\bar{H}_o$.

A further difference exists between the regions of Figure 1. At VHF, the quality factor, Q, is quite low for pure spin wave modes (on the order of 100 for pure YIG), quite high for the elastic system (10^4 - 10^6), and between 10^2 and 10^6 for the coupled magnetoelastic system.

The Q of the subharmonic mode determines the selectivity of the FSL, in that the linewidth of the subharmonic mode is $\Delta\omega = \omega/Q$. The selectivity has been defined as the half linewidth in Hz (Reference 2). The subharmonic mode amplitude has a Lorentzian dependence with respect to half the frequency of the applied signal. If the linewidth, $\Delta\omega$, is sufficiently small, each input frequency will essentially generate only its subharmonic. This is the mechanism by which frequency-selective limiting can be obtained. Assuming that the mode density is high enough to approximate a continuum, the independence of input signals (one or several of which may be large enough to be limited) can be measured in terms of the subharmonic magnetoelastic mode linewidth.

The basic FSL is constructed as shown in Figure 2 where the ferrimagnetic material has been placed in a resonant circuit and biased with an external magnetic field $\bar{H}_o$. To maintain a high elastic Q, the material used should be single crystal. To present low loss to the circuit at small signal levels, the bias field should be strong enough to make the material single domain. This will occur when the demagnetized external field has a component larger than the anisotropy field along an easy direction of the crystal. This is further discussed in the First Technical Report. For pure YIG, the magnetic crystalline anisotropy field is about 45 oersteds. This is quite high compared to the 30 oersteds required for operation within the spin wave manifold in the VHF range. Thus, anisotropy and dipolar interaction (proportional to M_s) make the low threshold high propagation angle spin wave regions of Figure 1 inaccessable.

The shape of the ferrimagnetic material is important in that a uniform internal field is desired. Other than a sphere, which will have a uniform internal field regardless of orientation, a rod could be used. However, in the case of the rod, anisotropy will distort the demagnetizing field unless the crystal is oriented with the symmetry axis is along the rod length. All experiments during the contract were performed using spheres.

I.3 CONCLUSIONS - FIRST SIX MONTHS

As a result of the first six months' efforts, the following conclusions concerning the optimization of the single-sphere circuit were presented in the First Technical Report (Reference 3):

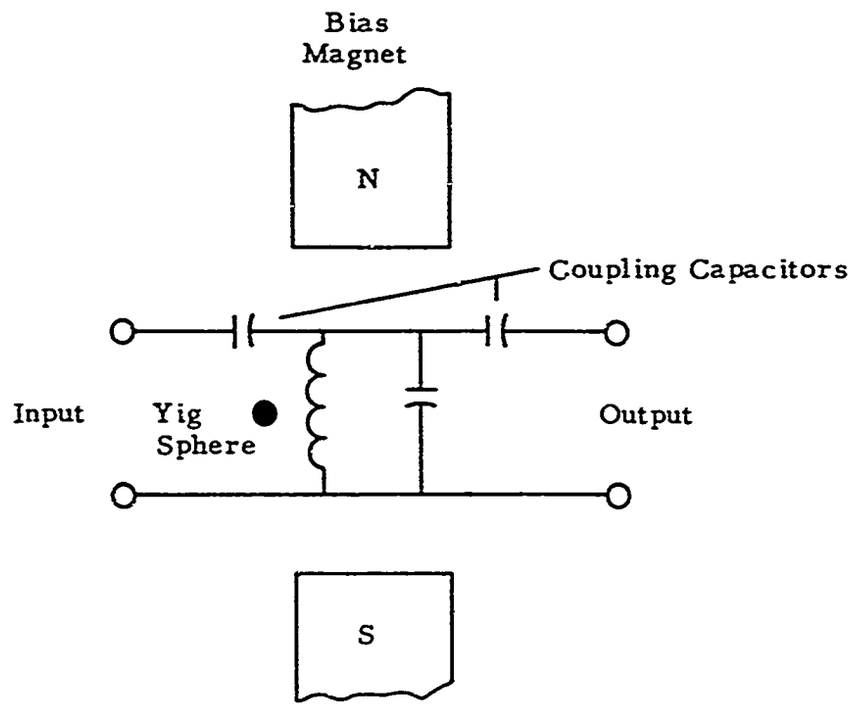

Figure 2 Basic Magnetoelastic Limiter (Parallel Pumped)

a. Material Choice

Pure YIG, YIG:Ga, Lithium Ferrite, Europium Iron Garnet, and Barium Zinc Manganese Ferrite (ZnY:Mn) were tested for the limiter application. Pure YIG, YIG:Ga, and Lithium Ferrite exhibited the widest dynamic ranges (15 to 20 dB). Pure YIG and YIG:Ga exhibited the lowest threshold powers (0 to + 20 dBm). A limiter using pure YIG heated to 100°C showed improved characteristics over the unheated case. Heating is not recommended for the final broadband limiter, since it would introduce severe design problems. Heavily doped YIG:Ga has shown the best overall limiting properties and is preferred for the final broadband limiter. The favorable properties of YIG:Ga are: reduced anisotropy, reduced M_s, reduced dependence of threshold on bias field, and increased mode density. All the above properties tend to improve the limiting properties. An unfavorable property of YIG:Ga is the increased temperature dependence of saturation magnetization. This leads to an increased temperature dependence of the d.c. demagnetizing field. In practice, this problem has been offset by the reduced bias field dependence of YIG:Ga.

b. Orientation

The test bias field direction for pure YIG is a [110] direction. For heavily doped YIG:Ga, both [110] and [100] directions were thought suitable (however, the [111] was found to be best during the last six months).

c. Damping

For pure YIG, the spin wave damping (linewidth) should be kept as small as possible in order to achieve a wide dynamic range. In this case, threshold and dynamic range are not found to be extremely sensitive to elastic damping.

For heavily doped YIG:Ga, the achievement of a low threshold and wide dynamic range requires a high elastic Q. Threshold is not sensitive to spin wave damping over a wide range of ΔH_k. Within this range, ΔH_k should be as large as possible to obtain maximum dynamic range.

d. Circuit Design

One of the most critical design parameters for the magnetoelastic limiter is the fill factor, which describes the effectiveness of coupling between the pump coil and the ferrimagnetic crystal. An improvement in this parameter by a factor of 2

would lead to a potential bandwidth increase by a factor of 4. Present fill factors are on the order of 0.1 to 0.2 compared to a theoretical maximum of unity. This is because the high fields near the coil wires are not coupling to the sphere.

The bandwidth of the limiter is determined by the degree of input-output coupling. As this coupling is varied, insertion loss, threshold power, and dynamic range also vary. The optimum coupling depends strongly on the required limiter dynamic range.

SECTION II

MATERIAL CONSIDERATIONS

II.1 MATERIAL PARAMETERS

The material chosen for the final breadboard model of the VHF-magneto-elastic frequency-selective limiter was gallium-doped single-crystal Yttrium Iron Garnet (YIG:Ga) as mentioned in Section I. The material was obtained from Airtron (Division of Litton Industries) in the form of spheres with the following specifications:

Diameter - 0.100 ± 0.01 inches
Saturation Magnetization - 200 ± 30 gauss
Maximum Linewidth - 10 Oersteds (better than 5 Oersteds as received)
Polished to a 0.3 micron finish
Sphericity better than 0.0001 inches (diameter variation)

Larger spheres are available and would provide higher mode density; however, the price was prohibitive. By using these larger spheres, the increased mode density would result in a reduction in relaxation oscillations.

II.2 DOPING

YIG crystals can be doped with either magnetic or nonmagnetic atoms. The basic crystal has a unit cell formed by five iron atoms distributed such that three are at tetrahedral sites and two are at octahedral sites. The material is ferromagnetic because the magnetic moment of the two octahedral atoms does not completely compensate the oppositely directed magnetic moment of the three tetrahedral iron atoms. As discussed in the First Technical Report, doping is desirable to minimize the effects of anisotropy. The process of doping YIG is complicated by being dependent on the material used. Doping with Ga involves replacing the Fe atoms with Ga atoms. The Ga mainly appears at the tetrahedral sites, but not entirely; therefore, replacement of one fifth of the Fe does not cause complete antiferrimagnetic compensation. Rather, the resulting magnetization is about 300 gauss. Because the Ga does go mostly to the tetrahedral sites, a comparitively small amount of Ga is required to provide a specific lowering in saturation magnetization. Other materials such as aluminum do not have the high affinity for the tetrahedral sites, and much more is required; thus, the linewidth of the material is much broader.

By replacing the yttrium with a magnetic atom such as dysprosium, the saturation magnetization can be changed, but the losses of the spin system are much more strongly affected, and a broad uniform precession resonance line results. Addition of a very small amount of magnetic atom would increase the rate at which energy is coupled from one portion of the YIG to another (increased spin-spin interaction) and this could reduce any problems of local heating resulting from the low heat conductivity of the YIG. Magnetic atom doping would make the material handle higher power without local heating phenomena and is further discussed in Sections II.7 and VIII.

Replacing the Fe with Ga lowers the Curie temperature (temperature above which the saturation magnetization is zero), whereas replacing the yttrium with a magnetic atom raises the antiferromagnetic compensation temperature. For YIG:Ga with magnetization of 200 gauss, the Curie temperature is about 130°C, whereas for pure YIG, the Curie temperature is about 275°C.

The highly doped (saturation magnetization of 200 gauss) YIG:Ga was chosen to maximize the dynamic range while maintaining a reasonably low threshold (see Reference 3 for relationship between dynamic limiting range and threshold power level). The material magnetic losses are high, but the magnetoelastic modes are mostly elastic such that subharmonic mode Q's of more than 10^4 were found. The FSL selectivity usually found was 3-5 KHz at 200 MHz (see Section VI).

The high doped YIG:Ga is not particularly sensitive to orientation when parallel pumping (rf and dc magnetic fields parallel) is used, orienting along the easy direction makes the FSL quite insensitive to vibration.

II.3 SURFACE CONDITION

The surface of each sphere was polished with a 0.3 micron abrasive to prevent random phonon-magnon scattering at the YIG-air interface. This surface preparation aids in keeping the magnetoelastic Q high. Prior to use the spheres were cleaned in a vibrating Freon bath and other than the glass supports, the spheres touch nothing. Contact with the coils was found to decrease the mode density and make relaxation oscillations more prevalent.

The air touching the remaining surface of the YIG:Ga sphere limits the elastic quality factor, Q. Since the FSL operation used mostly elastic magnetoelastic modes, evacuating the region around the spheres would probably reduce the threshold; however, this was not verified by experiment (see Section VIII).

Using a helium atmosphere, the FSL could be operated at about 3 to 5 dB higher power level without showing effects of heating. In the breadboard models, the encapsulation in helium was avoided to minimize the complexity.

II.4 TEMPERATURE EFFECTS

Changes in temperature will cause a small shift in the limiting threshold and a nearly negligible detuning of the FSL passband. The variations of saturation magnetization (M_s), anisotropy, (K_1) and linewidth (ΔH_k) with temperature are sketched in Figure 3. Variation of magnon losses with temperature is mainly in the liquid-atmosphere temperature region, where the losses are governed by the dopant sublattice. Since the FSL operates with mostly elastic modes, variations in magnon losses can be neglected. The variation in M_s as a function of temperature will cause a subsequent variation in threshold level. The variation in anisotropy can be neglected in the doped YIG:Ga because the threshold is mostly independent of K_1.

In summary, the only serious temperature effect (when YIG:Ga is used at VHF) is the variation in saturation magnetization. In design, one could minimize this effect by appropriate choice of the type dopant; taking advantage of the operating region being mostly elastic, some of the dopant could be magnetic so that the antiferromagnetic compensation temperature would increase. The resulting magnetization curve would be of the form of Figure 3d where the slope of the magnetization curve is quite small in our operating region. This type material would also have reduced relaxation oscillation effects (see Section II.7).

II.5 REQUIRED MAGNETIC FIELD

To minimize the phonon-magnon scattering (losses) the material must be all one domain. This requires an external magnetic field of sufficient magnitude such that the energy minimum (for the magnetization vector) caused by the crystalline magnetic anisotropy energy can be counteracted.

For YIG, this requires more than 10 gauss when the magnetic field is applied along an easy direction and as much as 90 gauss when applied along a hard direction. In Figure 4, the approximate orientation of major domains is shown as a function of the applied magnetic field for the cases where the applied magnetic field is along the [110], [111], and [001] crystal axes.

The magnetic field required to saturate the ferrimagnetic material can sometimes be so large that excitation of the low threshold modes may be prohibited. For example, for the ease of parallel pumping (see Section III) in YIG as in YIG:Ga, the external magnetic field required for

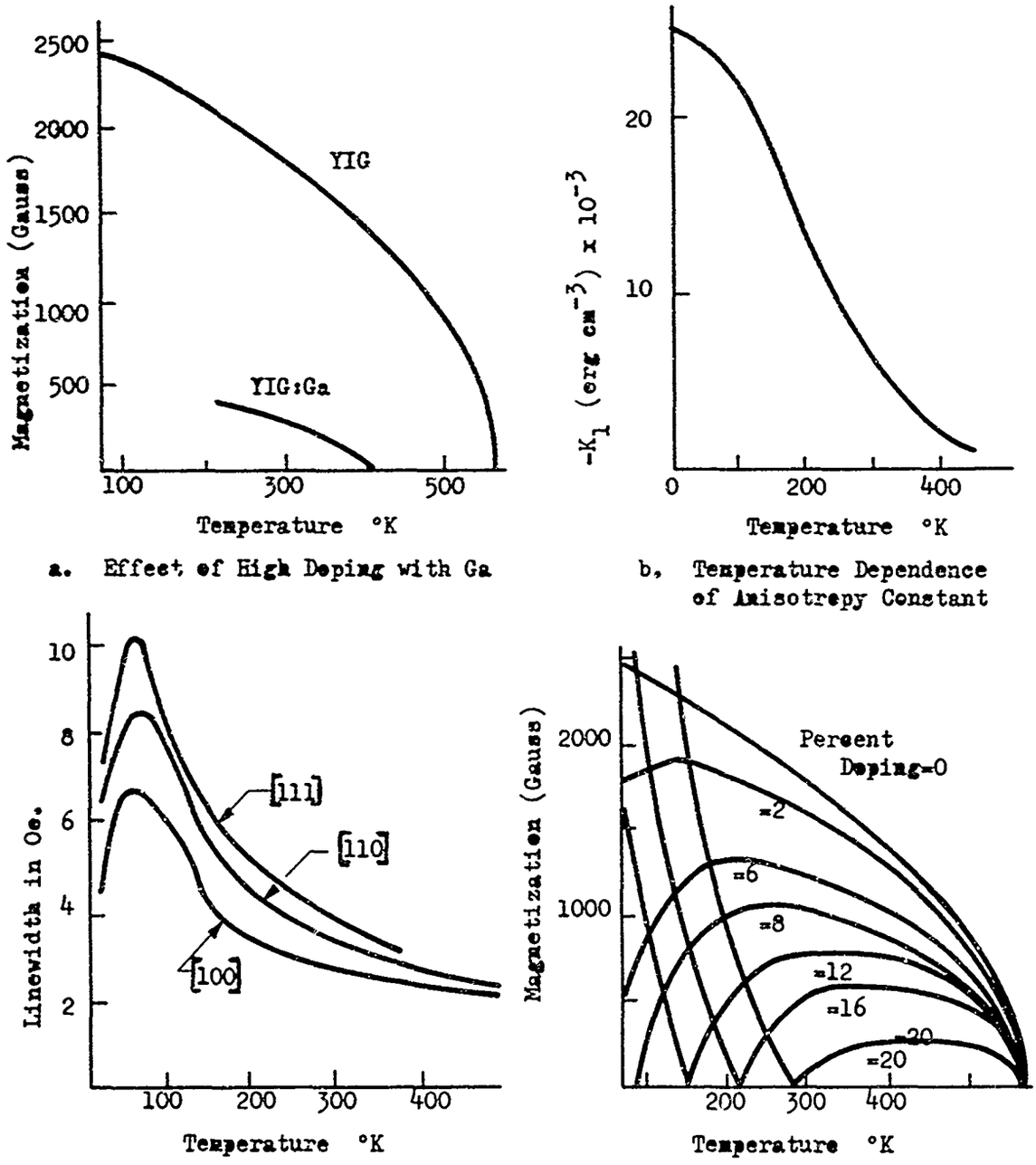

a. Effect of High Doping with Ga

b. Temperature Dependence of Anisotropy Constant

c. Temperature Dependence of Linewidth of YIG on Specific Orientation

d. Effect of Doping with a Nonmagnetic Atom in Percent of Fe Replaced with Ga.

Figure 3 Temperature Dependence of Material Parameters

saturation along a [001] direction is at least 2 K_1/M_s or about 90 gauss. The field (H) required to excite a spin wave frequency ω_k is contained in the expression

$$\omega_k = \gamma\sqrt{(H + H_{ex})(H + H_{ex} + 4\pi M_s \sin^2 \theta)}$$

where H = demagnetized external field

$\gamma/2\pi = (2.81)(10^6)$ Hz per Oersted

H_{ex} = Exchange field proportional to k^2

θ = Dipolar propagation angle

k = reciprocal wavelength

Very little exchange coupling is found at 200 MHz at minimum saturating magnetic fields, (H_{ex} can be neglected).

To excite a primarily elastic, magnetoelastic wave (above crossover) even with $\theta = 0$ (high threshold), we find that only about 70 gauss of demagnetized internal magnetic field is needed. To operate with a low threshold ($\theta = \pi/2$) mode, less field is required if the same k is desired.

In neither case will pure YIG be saturated if oriented along the [001] direction. By orienting the material along the easy axis, the internal field required for saturation reduces to less than 15 gauss. Pure YIG can then be operated at small angles θ (see experimental results presented in the First Technical Report, Reference 3).

With a material like YIG:Ga with saturation magnetization of 200 gauss, the low threshold modes can be excited for all orientations except those along the hard direction.

To minimize the sensitivity of the FSL to shock, the spheres used in the final breadboard model were oriented with the easy axis [111] along the external field direction. This allows the external field to maintain the crystal orientation and reduces the requirements imposed on the crystal holders. Also, the parallel pumping threshold power is low when highly doped YIG:Ga is used in this orientation.

II.6 MATERIAL SHAPE

The shape of the ferrimagnetic material is mainly restricted by the uniformity of the internal magnetic field required. To provide the best

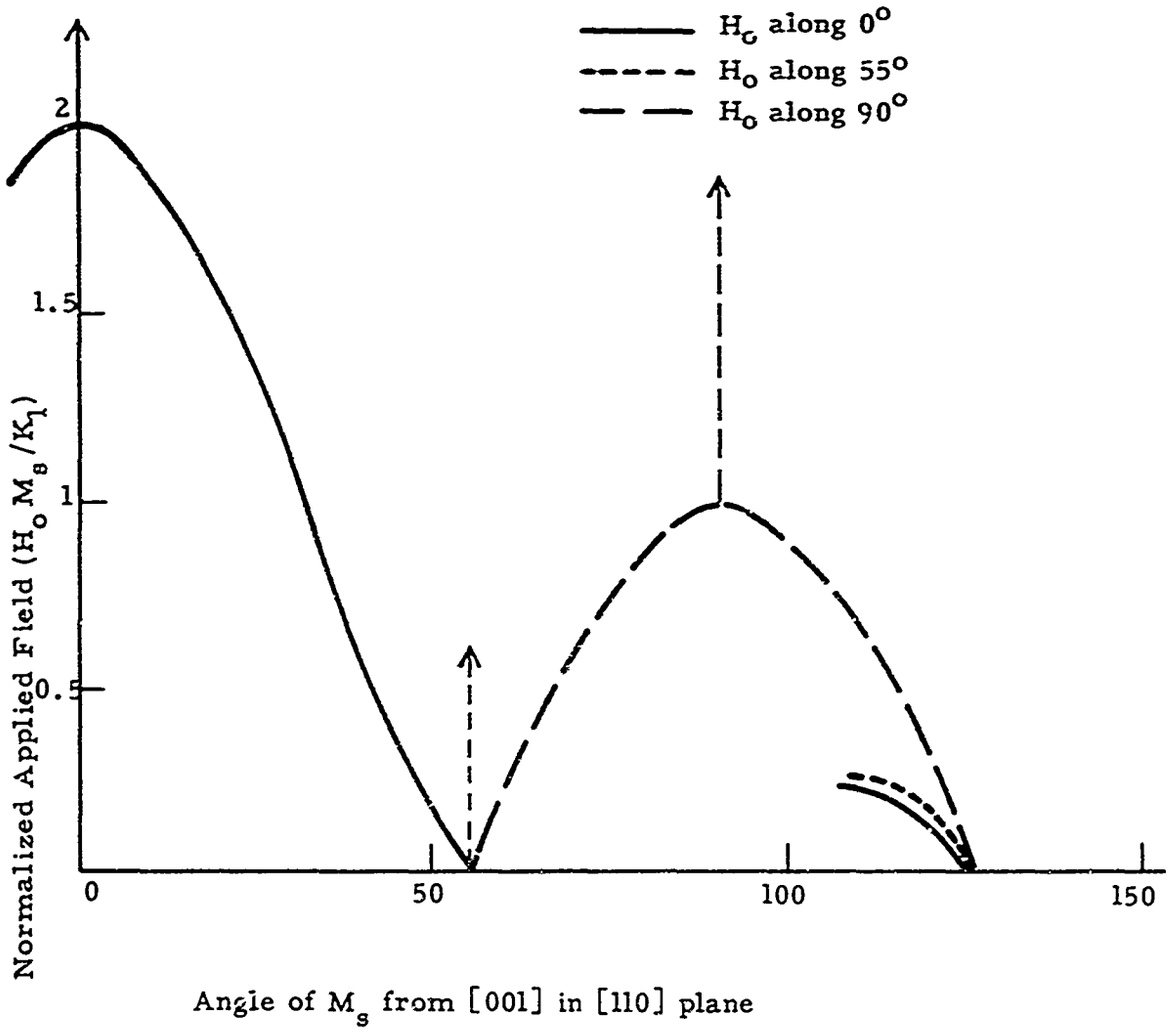

Figure 4 Approximate Domain Orientation with Respect to Orientation and Magnitude of Applied Magnetic Field H_o

coupling to a particular subharmonic mode, the dc magnetic field should be the same anywhere within the material. This will insure that the threshold will be uniform throughout the material for a particular mode; in addition energy can be supplied to the mode in all regions. If the internal dc field is too low in some region, the mode becomes more "spinwave like" (recall that operation is in region ③ of Figure 1). The spinwave mode losses are greater than the magnetoelastic mode losses, hence the apparent threshold of the low magnetic field region increases. The above inhomogenety also tends to reduce the mode density.

To obtain the uniform internal dc bias magnetic field, the ferrimagnetic material must be ellipsoidal or right circular cylinder shape. To make orientation measurements, a sphere was used because the sphere could be rotated to determine the dependence of the threshold on the orientation with respect to the crystal axes, without having to consider shape demagnetization factor effects. To make the initial material and orientation tests, small (about 0.025" diameter) spheres were used at UHF. Later, larger spheres were obtained and used to make orientation tests at VHF which allowed the threshold measurements to be made without undue interference from relaxation oscillations.

Except for price, a rod has certain advantages for the final model where the desired orientation is known. Rods are available with larger crystal volumes than spheres so that the mode density can be quite high. Rods have very small axial demagnetization factors so that saturation can be obtained at low external magnetic fields. One reason for not using rods was the concern that a threshold power level below 0 dBm could not be obtained (the rod has a high required threshold due to its size, but could possibly be placed within a coil to obtain a better fill factor than when using a sphere). After the appropriate doping and orientation studies had been conducted, several rods costing $500 each could have been ordered for use in a FSL model; however, the price was considered prohibitive.

II.7 NONLINEARITIES

Nonlinearities will occur when, from a classical point of view, the magnetization vector is precessing at angles with respect to the applied bias field. This phenomena results in a heating of the YIG:Ga and has been observed at FSL input powers exceeding one half watt. This nonlinear effect was considered in the First Technical Report.

A second type nonlinearity has been observed in the operation of the frequency selective limiters that use parametric subharmonic generation. In the coincidence mode type FSL operating in S-band, this type nonlinearity produced a "noise" on the limited output (see Reference 6).

In the VHF FSL test models constructed under this contract, this same type noise was found. Its characteristics are such that the term, "Relaxation Oscillation" has been used to describe the effect. Due to the low (VHF) operating frequency and the relatively small crystal dimensions, the mode density is low. Recall that the limiting action involves exciting a particular subharmonic mode. Apparently due to a local crystal heating caused by the energy being coupled to the subharmonic mode, the mode structure shifts and the coupling shifts to another subharmonic mode. The switching (or shifting) between subharmonic modes requires a new mode to become excited, causing a variation in the limited output power. Depending on the mode structure available to the subharmonic energy, various oscillation frequencies and amplitudes are observable.

As found when making intermodulation measurements, the relaxation oscillation in band noise is more than 30 dB below the signal. The effect should be further reduceable by adding a small percentage of magnetic atoms (probably less than 0.01%) to the YIG:Ga to increase the heat conductivity (through the added spin-spin coupling) at the expense of increasing spinwave losses. Since the FSL operates with subharmonic modes that are mostly elastic, this should not degrade the selectivity.

II.8 MODE DENSITY

The density of modes effects the FSL dynamic limiting range and also the unwanted relaxation oscillation (limiting noise). The factors effecting the mode density are:

a) Crystal size
b) Crystal orientation
c) Crystal support and surface damping

The effect (useful) modes are those magnetoelastic modes of the crystal that are of low threshold and that have high quality factors (Q_s). Modes that are damped by a strong coupling to a loss at the surface (such as would be caused when the crystal touches a wire) are not useful due to their high threshold and low Q.

The effect of the crystal size on mode density was discussed in Reference 3 where the expected mode density was shown to be proportional to the crystal volume. This mode density is also modified by crystal orientation because a crystal (e.g. pure YIG) can be oriented so that only certain types of modes can propagate.

SECTION III

PUMPING DIRECTION

Nearly all experiements were conducted using parallel pumping, but transverse pumping was also considered. The terms transverse pumping and parallel pumping arise from the relative orientations of the DC and time varying magnetic fields that are applied to the YIG:Ga sphere.

III.1 PARALLEL PUMPING

In the case of parallel pumping, the incident time varying energy is parametrically converted to the subharmonic mode frequencies due to the nonlinear interaction of the magnetization (spin system), the dipolar propagation direction, and the applied time varying field (through the crystalline magnetic anisotropy). This nonlinear coupling can be viewed as causing an elliptical precession of the magnetization vector around the DC bias magnetic field. Although transfer of energy directly to the subharmonic frequencies can occur without this elliptical precession (coupling by a dipolar interaction as shown in Reference 4), the most simple mental picture depicting the energy transfer mechanism does utilize anisotropy and ellipticity. With most crystal orientations, the magnetization vector precessing around the direction of external bias magnetic field (Z-axis) would make an elliptical trace in the x-y plane due to the crystalline anisotropy (see the First Technical Report). If the precession frequency is $\omega/2$, there is a time varying component of magnetization at ω along the z axis. Thus energy coupled into the system at ω can pump the precessing magnetization through the existance of anisotropy.

Although parallel pumping was discussed in the First Technical Report, recent work in the field has been done by Schloman (Reference 4). He calculated the threshold rf magnetic field (applied to a magnetic material parallel to the bias DC field) required to excite the subharmonic magnetoelastic modes. The analysis was more general than previously attempted by Comstock (Reference 5) in that the threshold was calculated for an arbitrary angle of propagation with respect to the bias field. Both longitudinal and transverse elastic waves were considered. Schloman restricted his attention to magnetoelastic waves that are mostly elastic (our case) and when magnetic losses are small and anisotropy can be neglected. The resulting threshold field was given

$$h_{th} \cong \frac{\omega}{\gamma \sigma T_e} \qquad \text{(III-1)}$$

where

$\sigma = \gamma B_2^2 / C_{44} M_s$

ω = pump frequency

γ = gyromagnetic ratio

T_e = elastic relaxation time

B_2 = magnetoelastic coupling constant

C_{44} = shear modulus

M_s = saturation magnetization

The results of his analysis indicate that if the subharmonic mode frequency is below the crossover frequency (spinwave curve of particular propagation angle crosses elastic curve in Figure 1), the threshold for subharmonic generation occurs for transverse waves that propagate at an intermediate (and typically small) angle with respect to the applied field. For our case where the subharmonic mode frequency is above the crossover frequency, Schloman agrees basically with the prediction and findings (Reference 3) that the lowest threshold is for transverse waves having $\theta = \pi/2$.

It was found during this contract that the $\theta = \pi/2$ waves cannot always be excited at low operating frequencies. This was true even in a highly doped crystal where direct anisotropy effects on the threshold could be neglected. As shown in Section II, the applied DC bias magnetic field required to make the material single domain (as is required to prevent high magnetoelastic losses caused by collisions at domain boundaries) is sometimes larger than that required to operate in the $\theta = \pi/2$ mode. as discussed in Section II.5, operation with highly doped YIG:Ga relieves this situation.

III.2 TRANSVERSE PUMPING

In the case of transverse pumping, the off resonance excitation of the uniform precession (k = 0) resonance is used to provide large fields within the YIG, and this energy is then coupled to the subharmonic mode (of the input frequency) through nonlinear interactions similar to those involved in parallel pumping. The use of the uniform precession mode can provide quite low thresholds if the frequency of the uniform precession resonance is not too different from the applied frequency. However, orientation of the crystal is important for VHF operation using transverse pumping because the orientation determines the bias

field required for saturation (thereby establishing the uniform precession resonance frequency), and the orientation determines the coupling to the uniform precession mode.

Uniform precession resonance occurs at a frequency ω_R where

$$\omega_R = \gamma\sqrt{(H + N_x M_s)(H + N_y M_s)} \qquad \text{(III-2)}$$

where N_x and N_y are the demagnetization factors in the x and y directions and where $H = H_o - N_z M_s$.

Even for the minimum magnetic field required for material saturation, ω_R is well above the VHF range. The amount of coupling to the uniform precession resonance will depend on the proximity of the operating frequency to ω_R and on the crystal orientation.

To obtain operation as close as possible to the uniform precession resonance, the material should be highly doped and oriented so as to saturate at the lowest internal field value (to lower ω_R of equation III-2). The coupling to the ω_R resonance is maximum when [110] direction is along both the bias and oscillating magnetic field directions. The net result is a high dependence on orientation even when using a highly doped crystal.

In summary, the final breadboard model did not use transverse pumping for the following reasons:

a) Transverse pumping increases sensitivity to mechanical shock because orientation for low threshold and high mode density is critical.

b) Only a slight reduction in threshold and increase in dynamic limiting range could be obtained from transverse pumping at VHF.

SECTION IV

CIRCUIT DESIGN

IV.1 CONCEPT

The initial design of the wideband model FSL was based on the test results obtained for the narrowband model was presented in Section I.3. The basic device operation concept was that when the input power was below the threshold level, the circuit could be treated linearly; however, above the threshold power level, the subharmonic generation of modes in the ferrimagnetic crystal would result in a large change in effective impedance of the element containing this crystal and a large change in input reflection coefficient would result. The subharmonic mode generated would produce fields that tend to cancel those being applied.

The time varying magnetic field in the crystal at limiting threshold is a function of the material, the dc magnetic field in which it is immersed, the relative orientation of the anisotropy axis and the time varying magnetic field direction. The circuit design effects the strength of the time varying magnetic field (for a given input power) and the coupling between the crystal and the circuit (usually measured by a fill factor).

To keep the input threshold power level low, the crystal must be placed in a resonant circuit element. To keep the fill factor high (and thereby keep the dynamic range[1] high), the time varying magnetic field must be confined to the crystal as much as possible. Since spheres were chosen for the material shape (as discussed in Section II.6), fill factors as high as 0.1 were found difficult to obtain (see Reference 3). Cavity designs at 200 MHz do not provide good fill factors for crystal spheres of 0.1" diameter and could not be used. Since the sphere could not touch other materials (without damping many modes and reducing the selectivity) it could not be embedded in a dielectric to concentrate the magnetic field in the sphere. The best configuration found was to place the sphere in the center of a coil where the coil length was slightly less than the diameter of the sphere, and where the coil diameter was 0.001" greater than that of the sphere. Some tests were made using flat (magnet-type) wire to get more of the sphere in the high magnetic field that is near the wire, but the coil-

1. Dynamic limiting range depends on the fourth power of the fill factor as shown in Reference 3.

support and sphere-coil alignment problems offset the ~3 dB reduction in threshold gained from the best flat wire coil tested. Another method tested to concentrate the time varying magnetic field within the sphere was to contour the coil cross-section to follow that of the sphere. The result was that the coil Q decreased and the alignment difficulty increased making the design impractical.

For the above reasons, the circuit chosen for the broadband FSL is that shown in Figure 5. This was the circuit used in obtaining the results of the First Technical Report and, after a series of necessary compromises, seems to offer the best results.

IV.2 BROADBANDING THE BASIC CIRCUIT

The bandwidth of the basic circuit was controlled by the coupling to the external circuit. As shown in Reference 3, an optimum coupling can be found such that the insertion loss is not excessive. As the bandwidth of the basic circuit was increased, the circuit Q decreased which raised the threshold and reduced the dynamic range by requiring higher power levels to be reflected by the circuit. The result is that a trade-off between the FSL dynamic limiting range (and threshold power level) and the bandwidth becomes necessary.

In summary, it was found impossible to broaden a single-sphere circuit sufficiently to obtain even a 5% bandwidth without reducing the dynamic limiting range to less than 6 dB.

IV.3 BROADBAND TECHNIQUES

Various broadband techniques were studied in an attempt to optimize the trade-off mentioned in Section IV.2 and obtain the best operating characteristics. The approaches studied included:

a) Transmission line circuits
b) Cascaded circuits using parallel resonances
c) Cascaded circuits using series resonances
d) Various forms of equal ripple filters

Each of these techniques and the results obtained are discussed below.

A lumped-constant transmission line was constructed. However, because the inductances were not actually resonant elements, the limiting threshold power level was well above one watt. For this reason, non-resonant broadband circuits cannot be used.

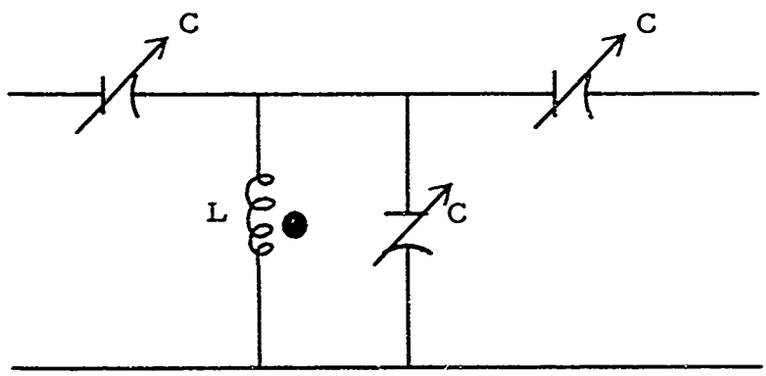

C = 1-10 pf

L = 0.045 μh

Figure 5 Basic Parallel Resonance Circuit FSL

Using the basic circuit of Figure 5, a cascaded model was constructed where three such circuits were used as shown in Figure 6. By making the coupling capacitors small (about 0.1 pf) between stages, the individual circuit resonances could be stagger-tuned to provide a much broader bandwidth. Both the isolation required to make the circuits independent and the stagger tuning of those circuits resulted in a difference in threshold power level for each circuit. The net effect is to cause a variation in threshold level and dynamic limitng range across the FSL passband. The testing of this circuit is discussed in Section VI.

To improve the effectiveness of the last circuits in a set cascaded-circuits, a low impedance model was constructed. Using a cascade of basic series-circuit elements, the circuit of Figure 7 was constructed. The interstage coupling and interstage isolation was accomplished with the use of impedance transformers and compartment-type construction. As will be discussed in Section VI, this model also had a variation in threshold and dynamic range across the band. The first few circuits did the most to change the input reflection coefficient while the later stages had little effect.

IV.4 TCHEBYCHEFF AND BUTTERWORTH FILTERS

In the design of a broadband FSL, the equal-ripple and maximally-flat filter design techniques were also considered. A broadband filter can be designed using either of the above concepts; however, in either case the size of the inductor required for resonance varied as much as an order of magnitude throughout the filter. To maintain a large fill factor, the coil must be nearly the same size as the sphere it enclosres. Thus, the inductor size is fixed and the normal Tchebycheff or Butterworth designs cannot be used.

IV.5 DESIGN OF EQUAL L BANDPASS FSL

The major problem encountered in using the normal Tchebycheff or Butterworth filter designs for the FSL is the large variation in required inductor sizes. Since the dynamic range decreases approximately as the fourth power of the fill factor, and since the large (0.1 inch diameter) spheres are required to maintain an adequate mode density, the design of the inductor is fixed. By making appropriate transformations of a given Tchebycheff or Butterworth low-pass prototype filter, an equal inductance bandpass filter can be designed (Reference 7).

The method for obtaining equal-inductance bandpass filters is based upon the idea of subjecting the network variable of the filter to a linear transformation under the restriction that the driving point impedance of the input port and the transfer impedance between the input and output

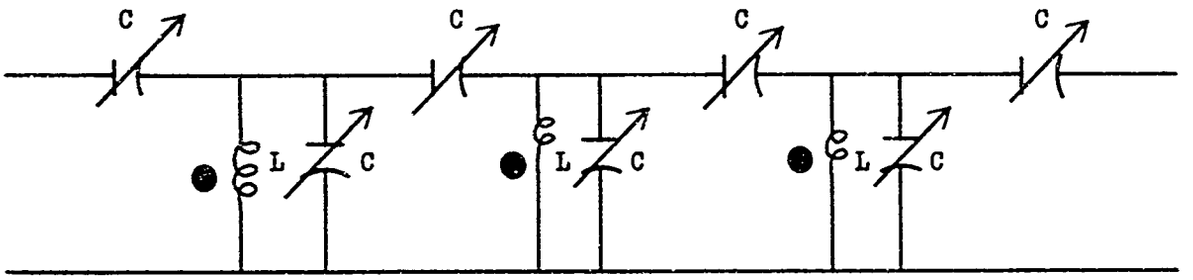

YIG:Ga Spheres denoted by ●

L = 0.045 μh

C = 1-10 pf

Figure 6 Three-Sphere Cascaded Parallel Resonant Circuit FSL

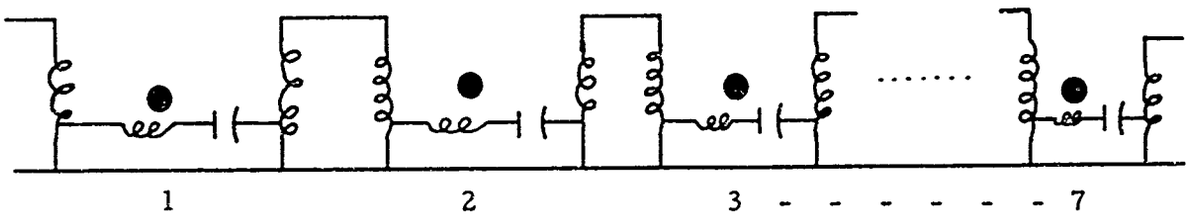

YIG:Ga Spheres denoted by ●

Figure 7 Seven-Sphere Cascaded Series-Resonant Circuit FSL

ports remain invariant. The mathematical details are covered in Guillemin (Reference 8) and will be omitted here. It should be pointed out that this technique is limited to the class of bandpass filters, obtained from lowpass filter prototypes which have all their transmission zeros at infinite frequency (e.g. Tchebycheff, Butterworth, and Bessel, but not elliptic filters). In particular, filters comprised of series inductors and shunt capacitors fall in the above category. The transformed bandpass network must have a structure in which all shunt inductors are flanked by an inverted L of capacitors, and all series inductors are preceded and followed by series capacitors.[2]

The low pass Tchebycheff or Butterworth prototype filter could have the form shown in Figure 8. Replacing each L by a series LC and each C by a parallel LC, we have the basic bandpass filter of Figure 9. The next step is to rewrite the circuit as in Figure 10 and to properly distribute the capacitance. The frequency is then scaled to the required center frequency, and the impedance is scaled to provide the proper input and output impedance.

With the aid of a computer, several designs were obtained for the circuit of Figure 11. These are listed in Table 1 where the generator and load impedance are equal ($R = R_g = R_L$). The value of inductance was taken as 0.08 microfarads (corresponding to the use of a slightly larger sphere) and the desired input-output impedance as R = 50 ohms. Tchebycheff lowpass prototype coefficients were assumed in the calculations.

The wider band circuits provided a higher input-output impedance and the capacitor values found were realizable. At 200 MHz, care must be taken in construction because the actual circuit values of components are modified by the presence of connecting wires and capacitor leads. It is recommended that the above circuits be constructed and evaluated for FSL application since they do appear to have some desirable features. Time limitations prevented the study of such filters on this contract.

---

2. The network whose inductances are to be equalized must be "conditioned" to this new form; this is often done by adding more capacitors in a manner which does not change the basic network. This step in the circuit design process is required because the new network is based on manipulation of a 2 x 2 admittance submatrix of capacitors in order to perform the necessary impedance leveling.

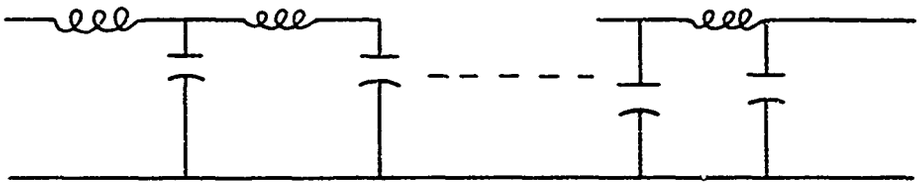

Figure 8 Basic Lowpass Prototype Filter

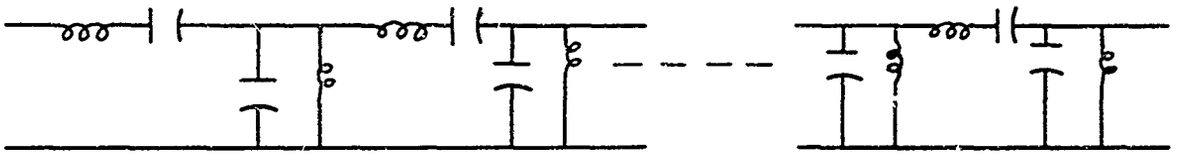

Figure 9 Intermediate Bandpass Prototype Network

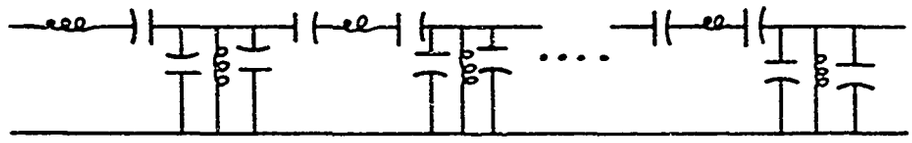

Figure 10 Conditioned Bandpass Filter Network

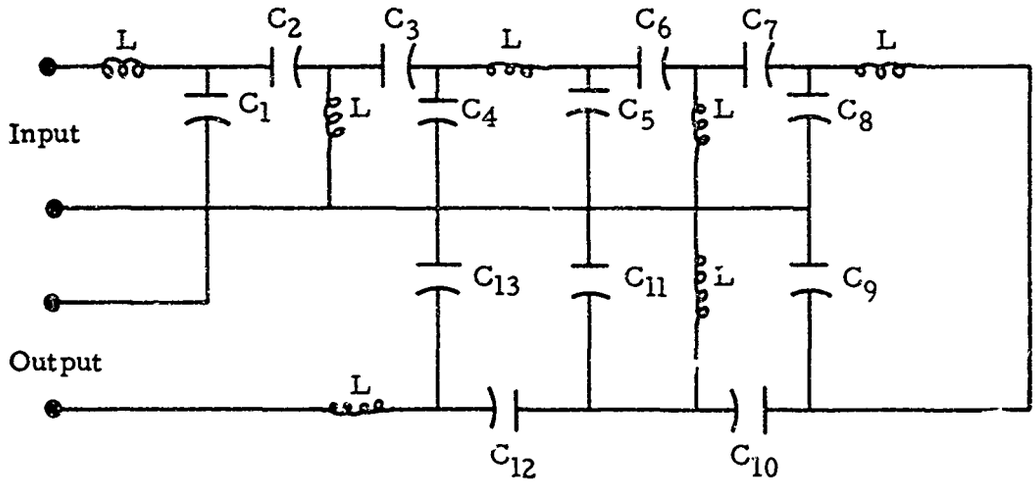

Figure 11 Normalized (Equal Inductance) Bandpass Filter

Case	1	2	3	4
Upper Cutoff Frequency (MHz)	210	220	300	300
Lower Cutoff Frequency (MHz)	190	180	150	150
Percent Bandwidth	10	20	Octave	Octave
Ripple (dB)	2	0.1	2	2
R (ohms)	3.5	17	26.3	52.6
L (μh)	0.08	0.08	0.08	0.16
C_1 (ppf)	7.4	6.8	4.0	2.0
C_2 (ppf)	0.5	1.2	3.1	1.5
C_3 (ppf)	7.9	7.9	8.5	4.3
C_4 (ppf)	140	59.7	14.1	7.1
C_5 (ppf)	7.9	8.1	6.5	3.2
C_6 (ppf)	0.4	1.0	3.8	1.9
C_7 (ppf)	7.9	8.0	7.4	3.7
C_8 (ppf)	144	64.2	12.7	6.3
C_9 (ppf)	7.9	8.0	6.8	3.4
C_{10} (ppf)	0.5	1.1	4.1	2.1
C_{11} (ppf)	7.1	6.0	2.8	1.4
C_{12} (ppf)	0.5	1.2	3.1	1.5
C_{13} (ppf)	7.4	6.8	4.0	2.0

Table I

Characteristics of Normalized Bandpass Filters

SECTION V

MAGNET REQUIREMENTS

The magnet required to provide the external bias magnetic field can be quite small. The field required is that necessary to make the material single domain (saturate the material) and to place the operating point in the magnetoelastic region ③ of the dispersion curves of Figure 1. The field required for saturation depends on the material shape (which determines the demagnetization factors) and on the orientation with respect to the applied magnetic field. These effects were discussed in Section II. For the highly doped YIG:Ga spheres used in the final models, the required external magnetic field was only about 170 gauss. This low field could easily be applied over a reasonably large region using a simple parallel plane magnet. An available 8" x 8" magnet, having two iron plates separated by 1" Alnico 5 permanent magnets at the corners, was magnetized. This magnet weighs less than 10 pounds and was used during the testing of the 7-sphere cascaded series resonant circuit model as discussed in Section VI. This FSL-with-magnet combination is picture in Section VI as Figure 30.

Based on tests of threshold power level variation with applied bias magnet field magnitude, small changes of the applied field will not significantly change the FSL operation.

Tests on YIG:Ga spheres with 320 gauss saturation magnetization indicated that more than a 50 gauss increase in external bias field is required to increase the threshold 10 dB (see Reference 3) in a worst case. This means that shielding of the FSL from external (constant or slowly varying) magnetic fields of 10 gauss or less is not necessary. Also orientation of the FSL in the earth's field is unimportant.

SECTION VI

TESTING

VI.1 DESIGN GOALS

The design goals were presented in Section I and are repeated here.

Frequency	150-250 MHz
Bandwidth	20% - One Octave
Insertion Loss	3 dB to 0.5 dB
Ripple	±2 dB to ±0.5 dB
Limiting Dynamic Range	15 to 30 dB
Magnetoelastic Q	400 to 10^7
Limiting Threshold	0 dBm to -20 dBm

The contract aim was to demonstrate that a highly frequency-selective power limiter could be constructed to operate at VHF with better characteristics than obtainable at contract outset.

VI.2 TESTING SINGLE-SPHERE CIRCUITS

During the first half of the contract period and well through the last half, single-sphere frequency selective limiter models were tested to determine the effect of material parameters and orientation on the selective limiting action. These single-sphere circuits were also studied to determine design criteria (in terms of the circuit parameters) necessary to broaden the FSL bandwidth. The effects of orientation, anisotropy, doping, and damping were determined during the first half of the contract, and the test results were presented in the First Technical Report. Although the doping selection at the end of the first half the program indicated intermediate doping, later tests indicated that a more highly doped sphere provided a higher dynamic limiting range and a higher mode density (reduced relaxation oscillation), for both parallel and transverse pumping.

The best single sphere FSL tested during the contract had the following characteristics:

Frequency	150-200 MHz
Bandwidth	2-3 MHz
Dynamic Limiting Range	15 to 20 dB

Subharmonic Q	$\sim 10^4$
Insertion Loss	8 - 12 dB
Threshold Level	< 10 dBm

Several problems existed with this model. The 15-20 dB of limiting could not be obtained everywhere within the band (without readjusting the bias magnetic field at each new frequency within band). Indications were that only certain mode clusters would provide good limiting. Secondly, the 15-20 dB of limiting was not constant, but varied in time as the ferrimagnetic material began to heat (internal losses) and the effective modes shifted in frequency allowing the amount of limiting to change.

The bandwidth was also quite narrow. The bandwidth of the single sphere circuit could only be increased at the expense of the dynamic limiting range and an increased limiting threshold (Reference 3). Transverse pumping was tried to reduce the threshold to allow increase in bandwidth, but the VHF transverse pumping and parallel pumping thresholds were found to be similar. To remedy the above problem, testing was directed toward the use of multiple spheres and stagger tuned resonant circuits to increase the bandwidth as will be discussed next.

VI.3 INITIAL TESTING OF MULTIPLE SPHERE CIRCUITS

The first results obtained for a multiple sphere circuit were for the case of two-spheres, each in parallel resonant circuits that were stagger tuned and cascaded as shown in Figure 12. The test results were as follows:

Frequency	200 MHz
3 dB Bandwidth	8 MHz
Insertion Loss	< 2 dB
Ripple	< 2 dB
Dynamic Limiting Range	10-15 dB
Threshold	+ 5 dBm
Subharmonic Q	$\sim 10^4$

The dynamic limiting range was more continuous across the band than obtainable with a single sphere FSL. A flat ribbon-like wire was cut from a silver plate and used for the coils containing the YIG.

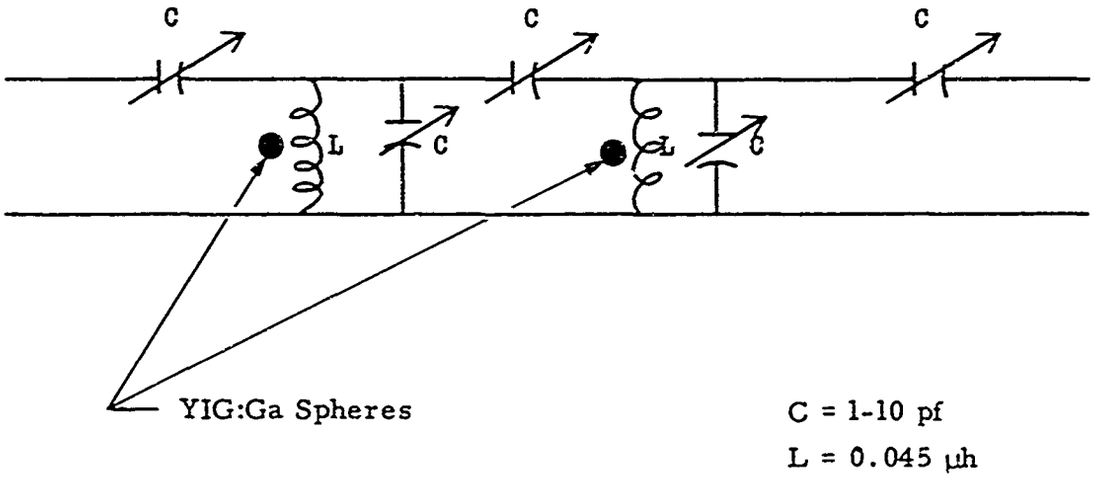

Figure 12 Two-Sphere Cascaded Parallel Resonant Circuit FSL

The ribbon wire allowed more of the strong fields to be concentrated in and near the spheres (providing an increase in fill factor), and lowered the threshold 1-3 dB. (In Reference 3, the dynamic range was shown to depend highly on the fill factor.) Using the flat wires, maintaining a 0.0005" clearance from the sphere was difficult and measurements were not repeatable. To make the coils more vibration insensitive, they would have to be carefully potted. This was avoided in the construction of the breadboard model for the sake of simplicity and to allow the circuit to be easily changed and studied.

Using three spheres in cascaded parallel resonant circuits, the best results were:

3 dB Bandwidth	17 MHz	8 MHz
Insertion Loss	2-5 dB	2-5 dB
Ripple	< 2 dB	< 2 dB
Dynamic Range	~ 10 dB	~ 16 dB
Threshold	10-20 dBm	10-20 dBm
Subharmonic Q	$\sim 10^4$	$\sim 10^4$
Frequency	150 MHz	191 MHz

using parallel pumping and conventional wire. The first circuit was found to provide most of the limiting. The stagger tuning of the circuit resonances (required for wide band operation) resulted in a higher apparent threshold for the downstream circuits due to the off resonance attenuation of the first circuit. The expected limiting dynamic range was also lower off the resonance of the first circuit because material internal heating was encountered (see Section II.7 and Reference 3). As a result of the above test, it was apparent that to lower the threshold, the individual circuits needed to have tighter coupling to the input power. In an attempt to lower the threshold, transverse pumping was again attempted. Note that the spheres being used have excellent doping for transverse pumping experiments (see Reference 3).

Using transverse pumping with the three-sphere cascaded parallel-resonant circuit, the limiting curves for two bandwidth settings were obtained as shown in Figures 13 and 14. Note that the narrow-band tuning produced an FSL which had a flatter limiting characteristic than when the circuits were further separated to broaden the bandwidth. This was because in the narrow band case there is less separation in individual circuit threshold power levels so that each circuit can produce limiting at nearly the same threshold.

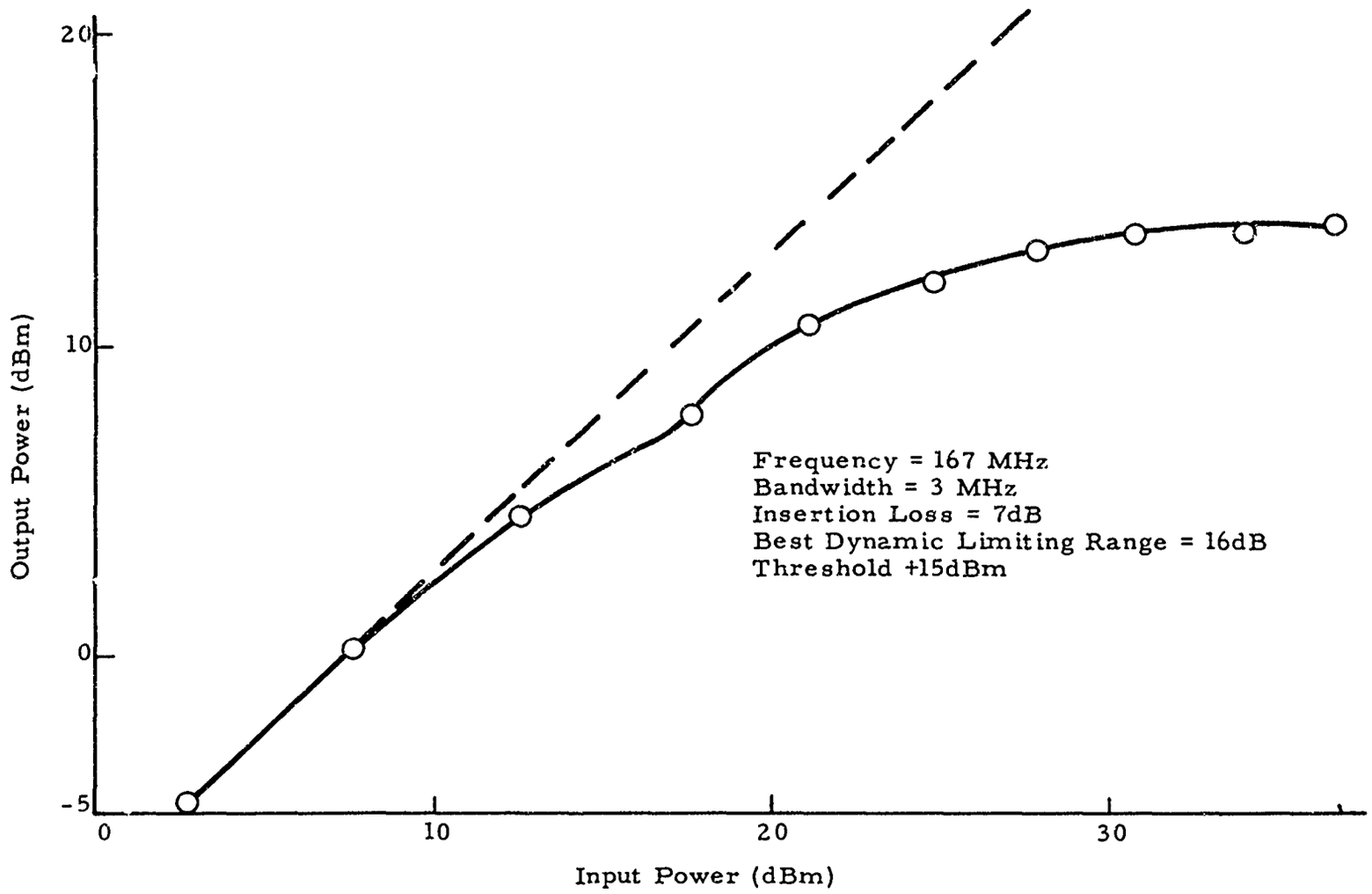

Figure 13 Limiting Curve for Case of Transverse Pumping with Three Sphere in Cascaded Parallel Resonant Circuits.

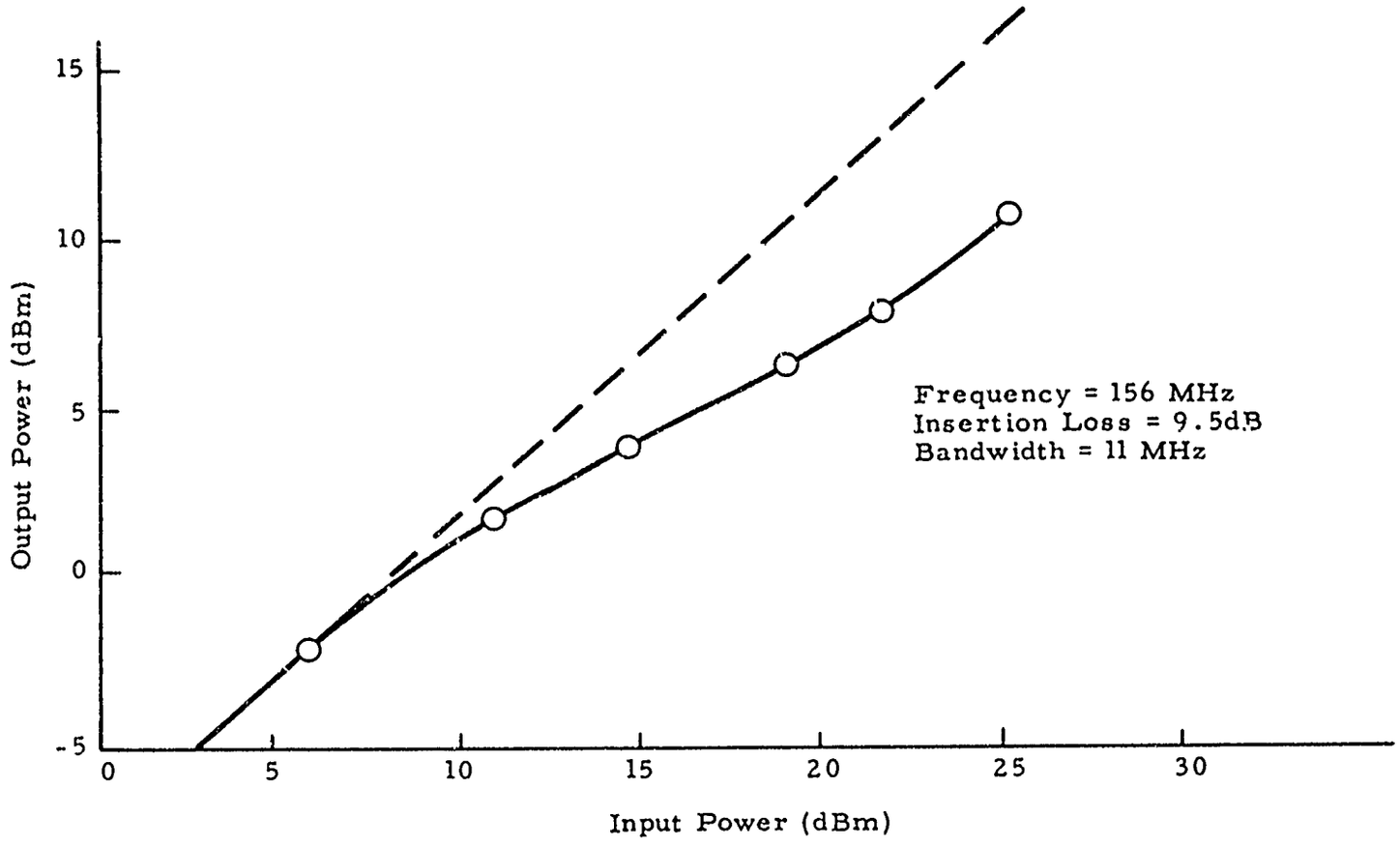

Figure 14 Limiting Curve for Transverse Pumping Wide Band Three Sphere Cascaded Parallel Resonant Circuit.

Parallel pumping using the same three-sphere cascaded parallel resonant circuit FSL resulted in the limiting curve of Figure 15. No particular advantage was found for either parallel or transverse pumping, so parallel pumping was chosen for use in the final models to remove stringent orientation requirements. Were the FSL constructed to operate at 400 to 800 MHz, the transverse pumping would probably have been selected because the input frequency would be closer to the uniform precession resonance frequency.

VI.4 TESTING FINAL MODELS

Two models were selected for test during the final contract phase. Based on tests made previously, the best broadband FSL's developed were: 1) the three sphere cascaded parallel resonant circuit model of Figure 6, and 2) the seven sphere cascaded series circuit model of Figure 7. The former had the advantage of lower insertion loss and wider bandwidth, and the latter had higher dynamic range.

VI.4a Testing Three-Sphere Model

The three sphere circuit of Figure 6, pictured in Figure 16, was tested (the YIG:Ga spheres can be seen, held by glass rods, in the small coils). The results are shown in Figures 17 through 26. The systems used for test are shown in block diagrams of Figures 27 through 29. The center frequency was set at 166 MHz. The -3 dB bandpass of about 11 MHz (from 160.4 to 171.2) is shown in Figure 18. For small signals, less than 2 dB ripple was obtained, and the phase shift across the band was linear (Figure 20). The dynamic limiting range was 8 to 12 dB. The threshold was below 0 dBm for only a small section of the band because the latter circuits had a higher threshold (due to low coupling to the latter circuits) as discussed previously.

The intermodulation results depict the frequency-selective limting potential of the device. Using the measuring apparatus of Figure 27, the results of Figures 23 and 24 were obtained. Note that for a large signal component 20 dB above threshold and a small signal 10 dB below threshold, the intermodulation products are more than 20 dB below the small signal (as seen at the FSL output) when the frequency spacing between the two components is as small as 60 to 90 KHz. Even for a large signal 30 dB above threshold and a small signal 10 dB above threshold, the intermodulation components are 10 dB below the small signal when the frequency spacing is more than 130 MHz. These extremely good intermodulation characteristics are a result of the selectivity (as shown in Figure 25 which is better than 3 KHz for most of the band. The intermodulation level was almost independent of the frequency at which it was measured.

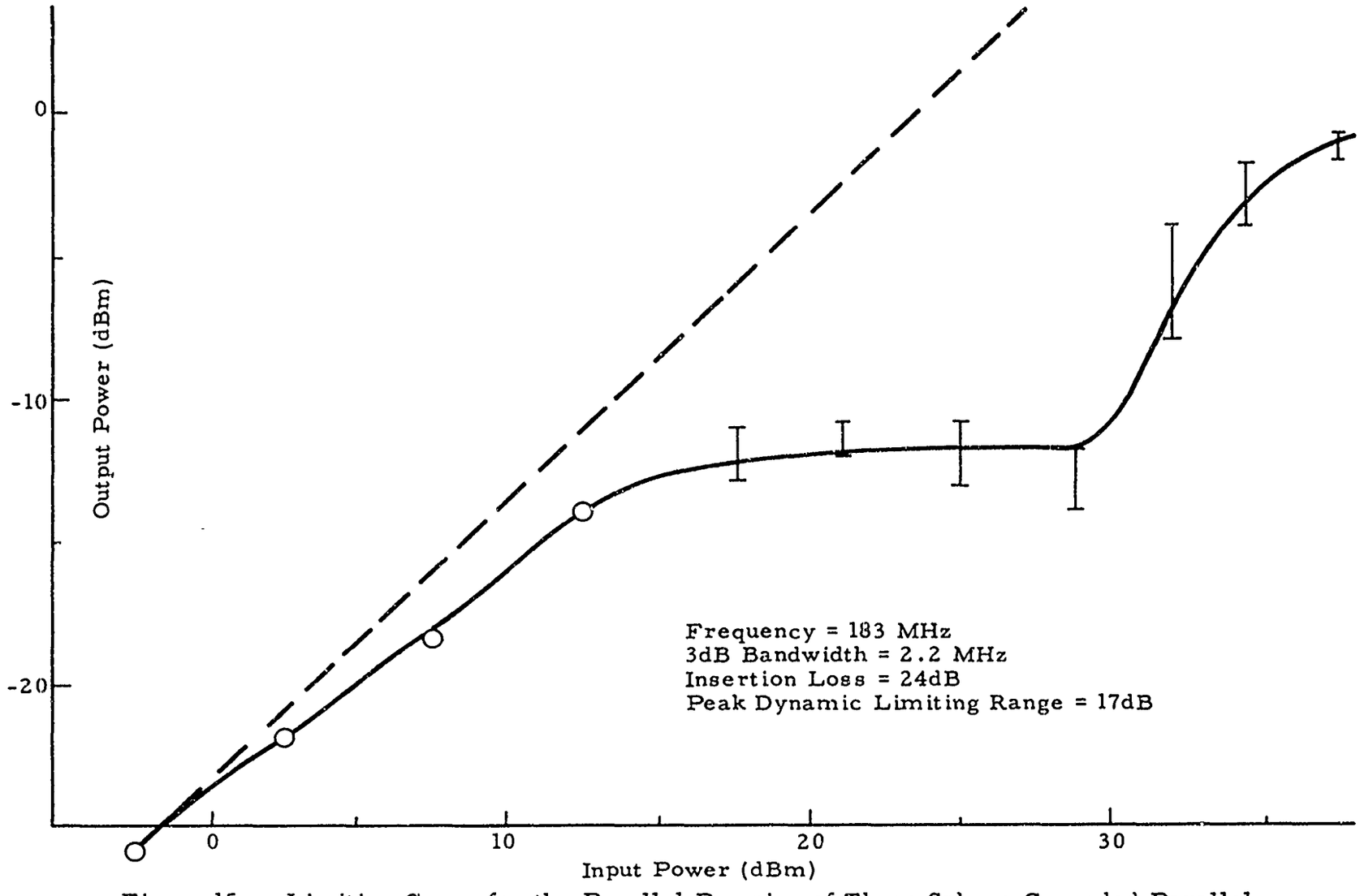

Figure 15 Limiting Curve for the Parallel Pumping of Three Sphere Cascaded Parallel Resonant Current FSL. Spread in data is due to heating.

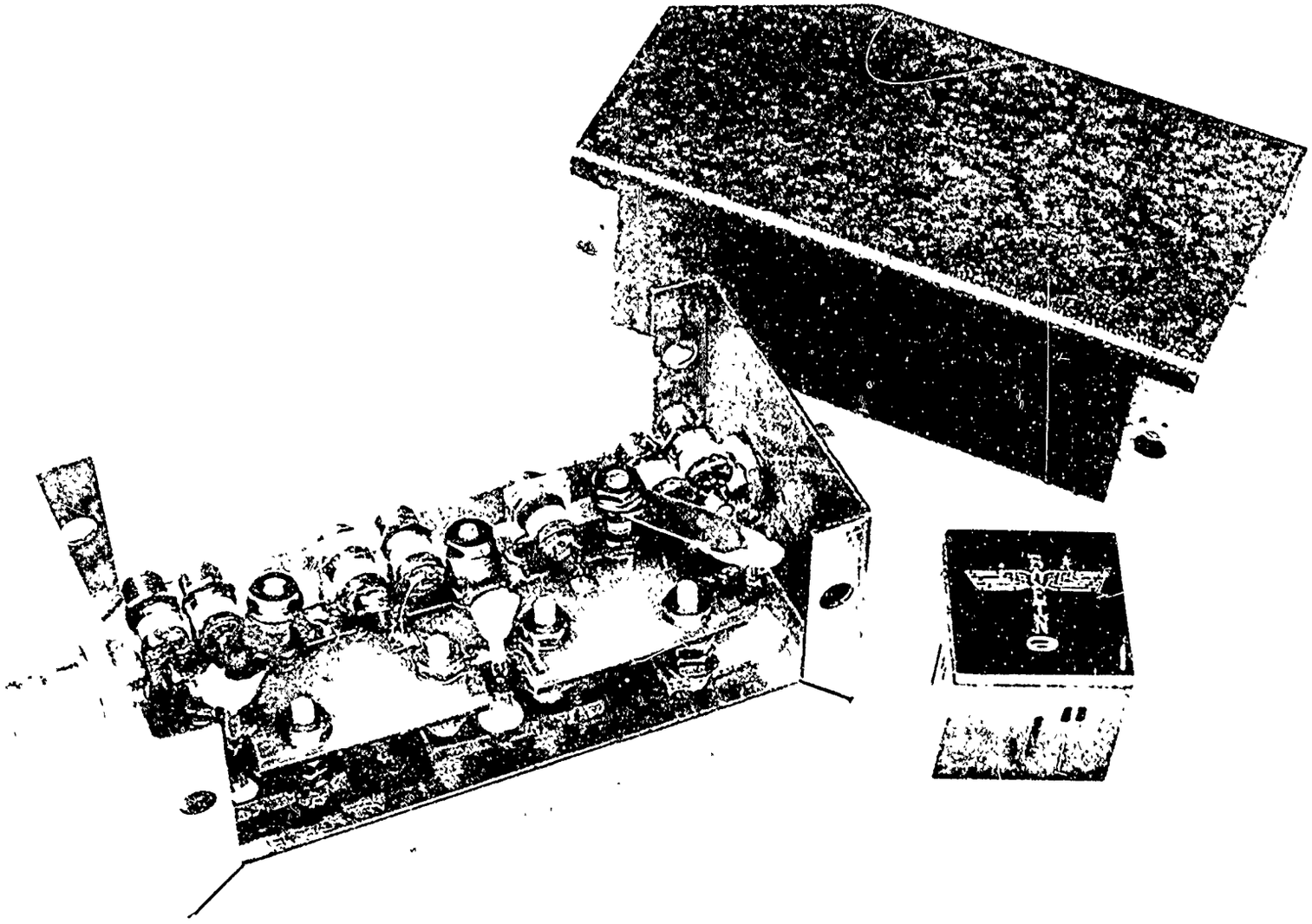

Figure 16 Picture of Three-Sphere Final Breadboard Model

Figure 17 Threshold of Cascaded Three-Sphere FSL

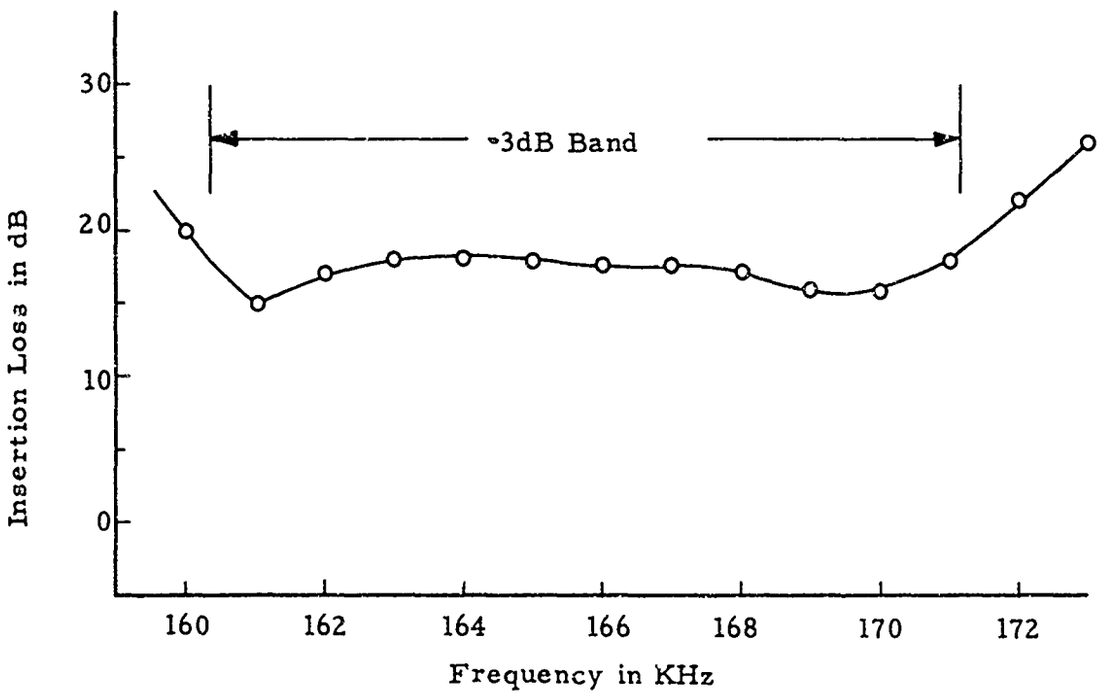

Figure 18 Small Signal Insertion Loss of Cascaded Three-Sphere FSL

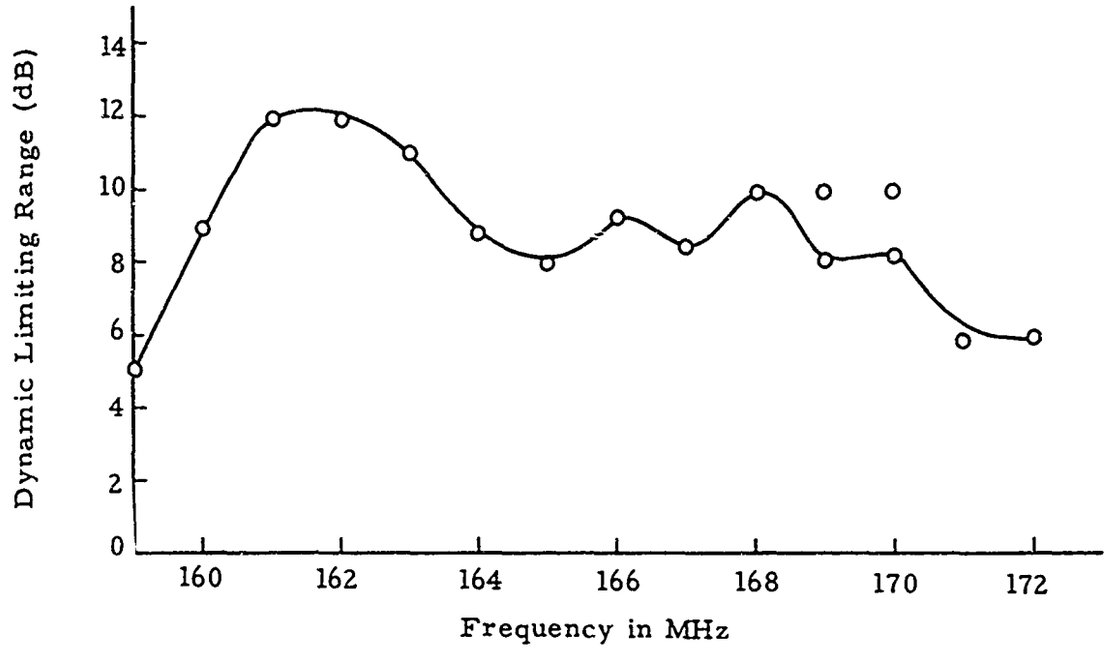

Figure 19 Dynamic Range of Cascaded Three-Sphere FSL

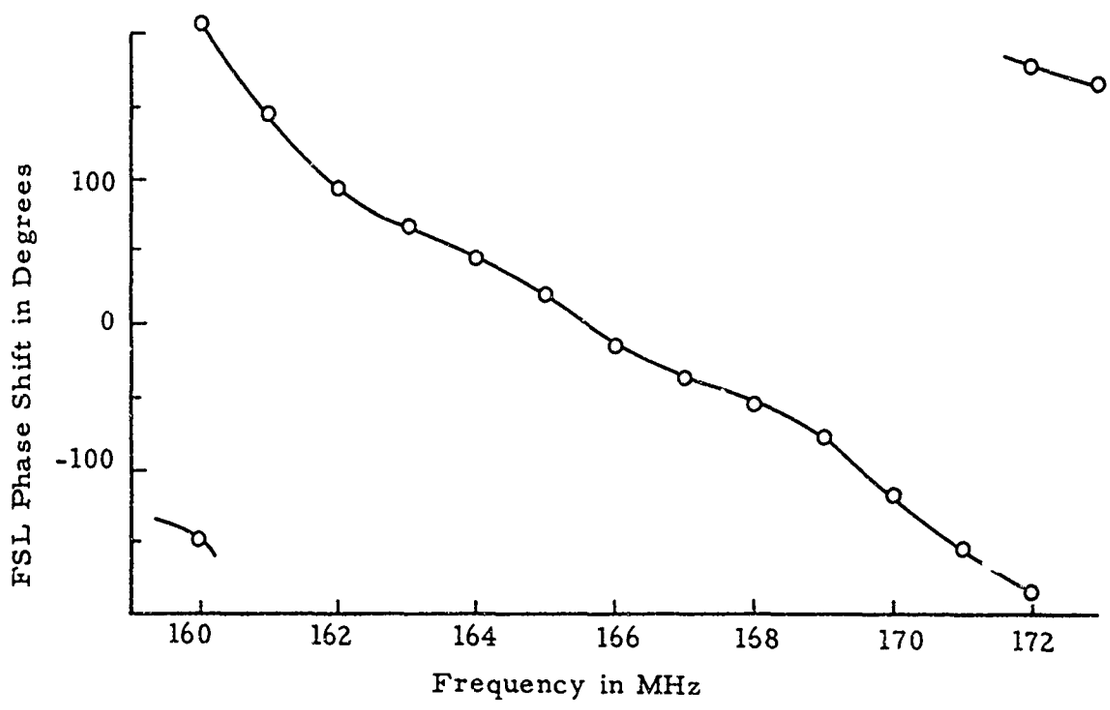

Figure 20 Phase Shift of Cascaded Three-Sphere FSL

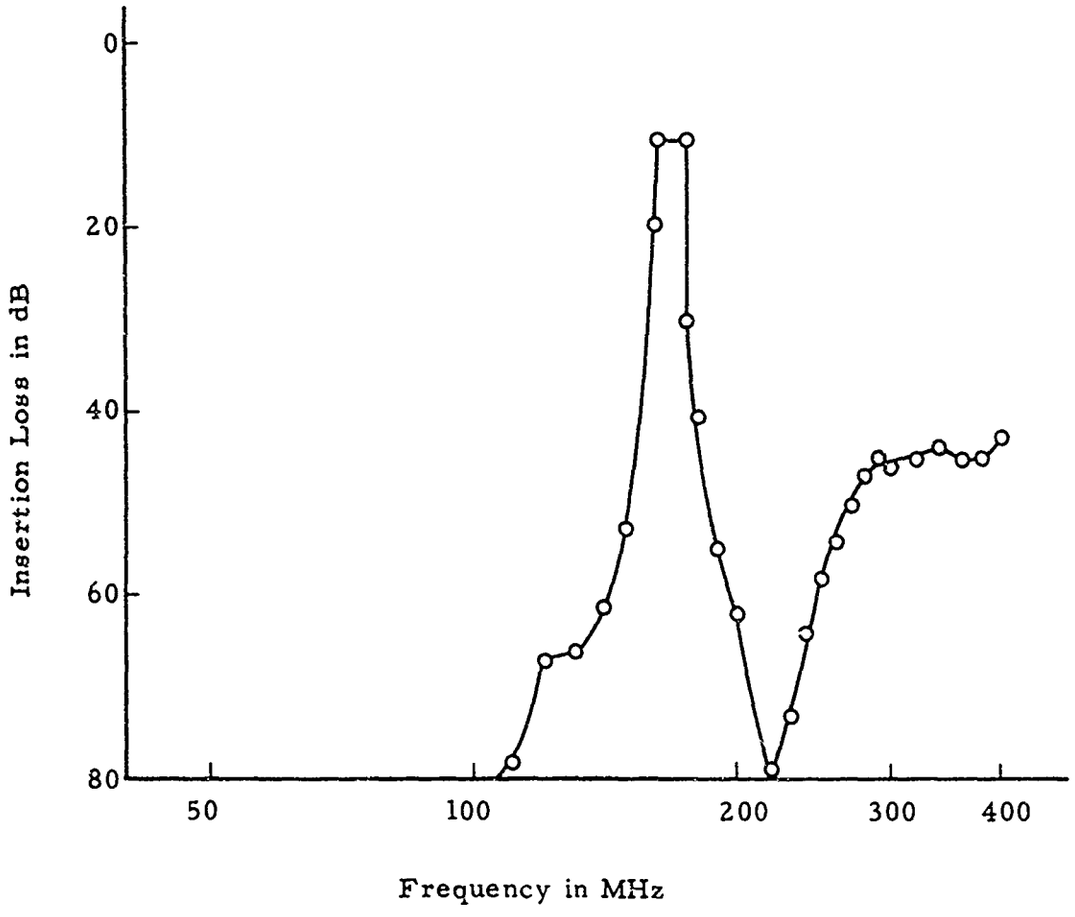

Figure 21 Small Signal Amplitude Response

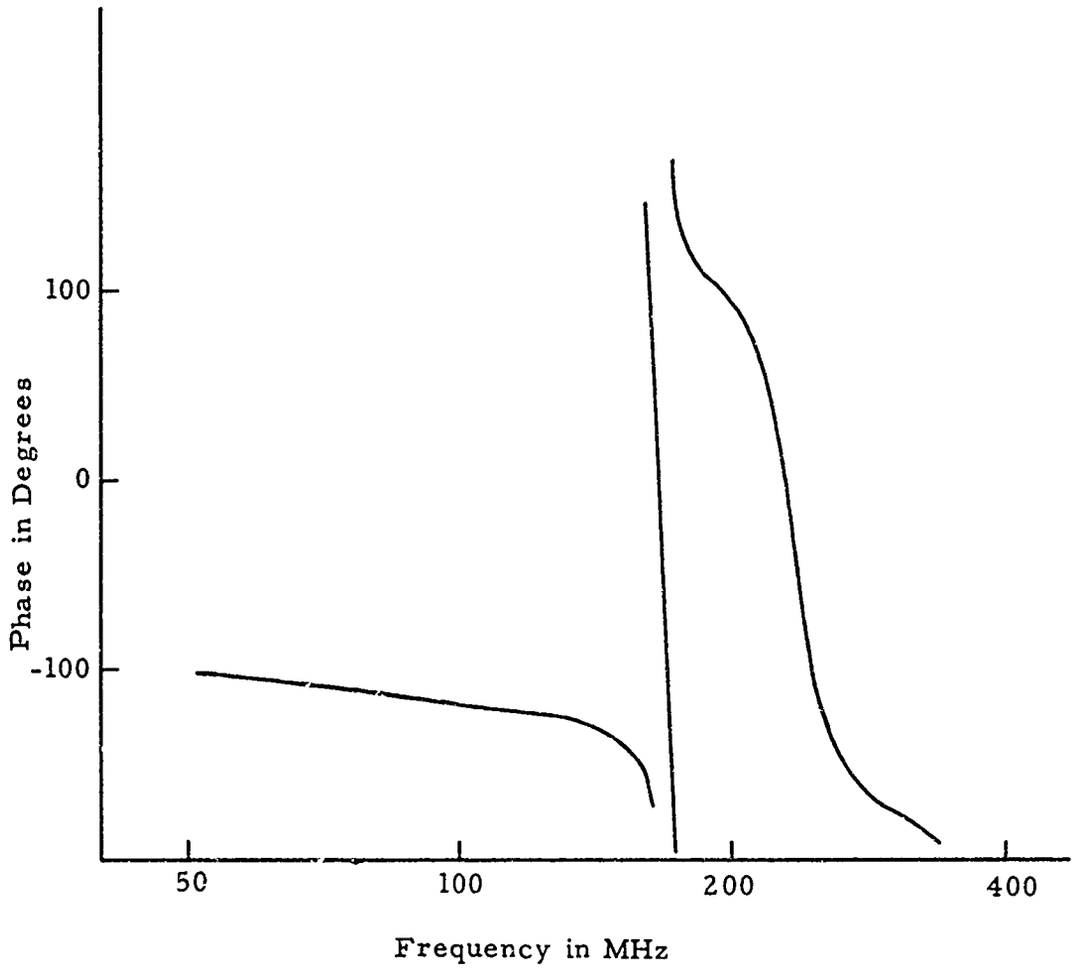

Figure 22 Phase Response of Cascaded Three-Sphere FSL

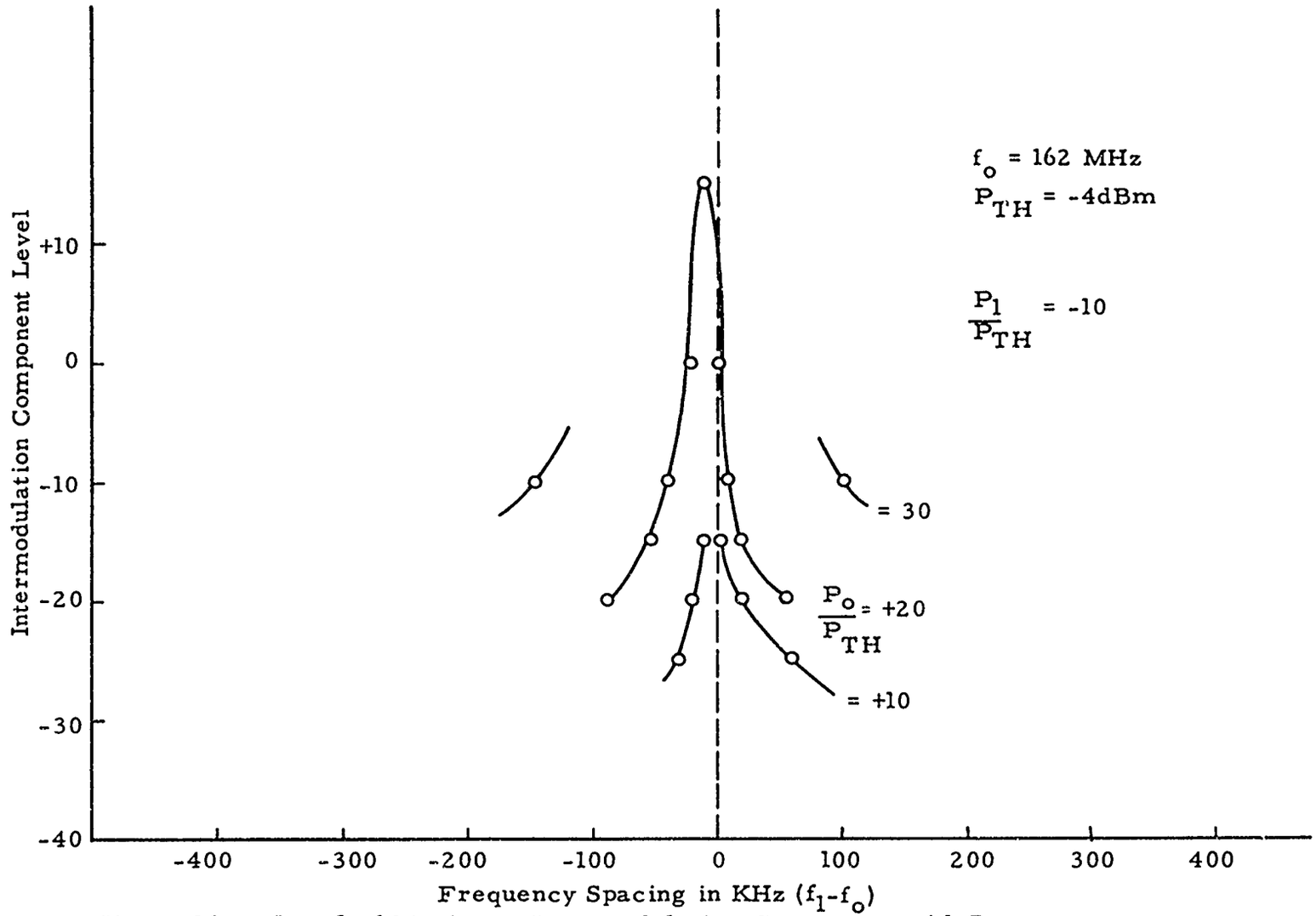

Figure 23 Level of Maximum Intermodulation Component with Respect to Level of Small Signal

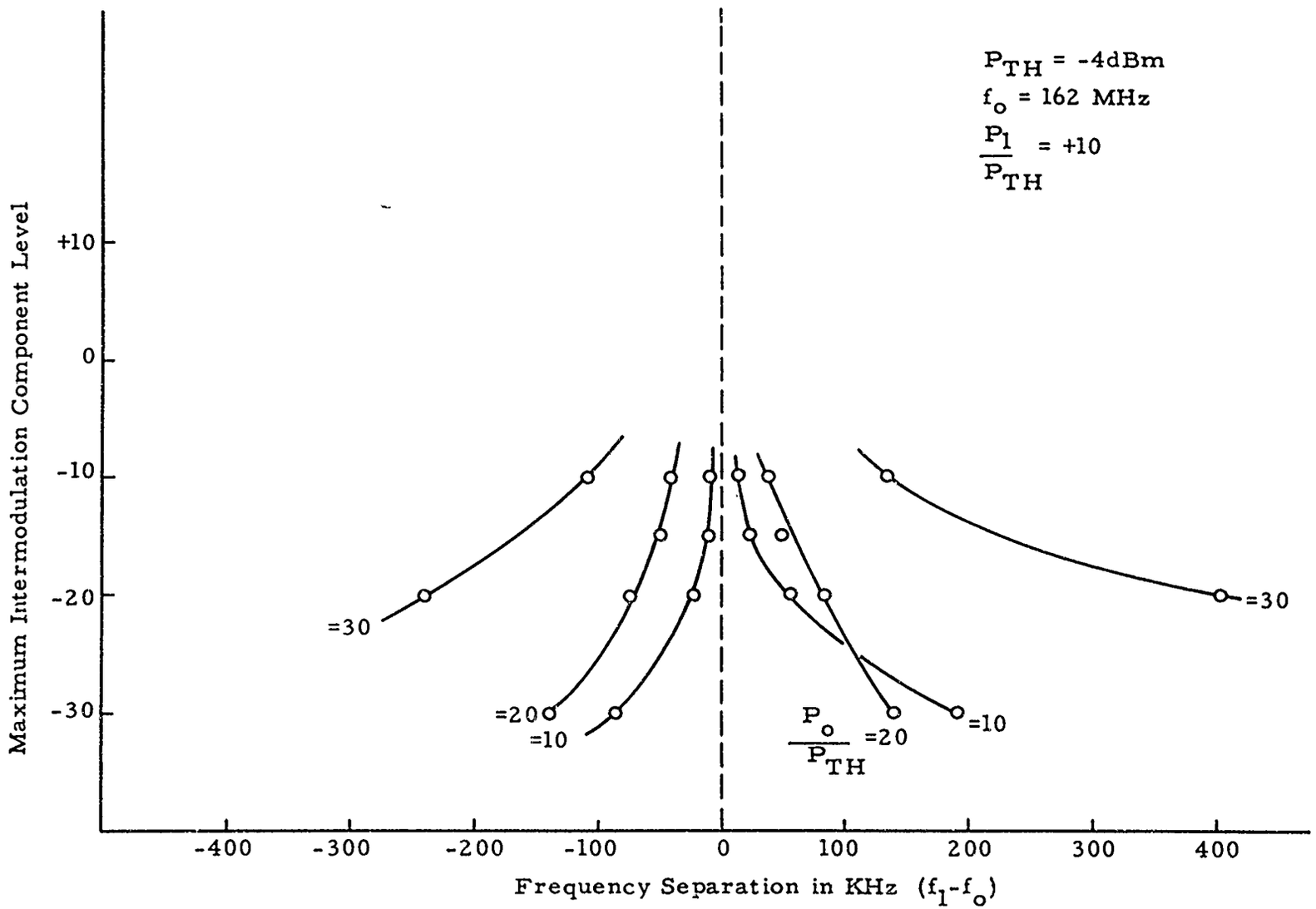

Figure 24 Level of Maximum Intermodulation Component with Respect to Suppressed Small Signal

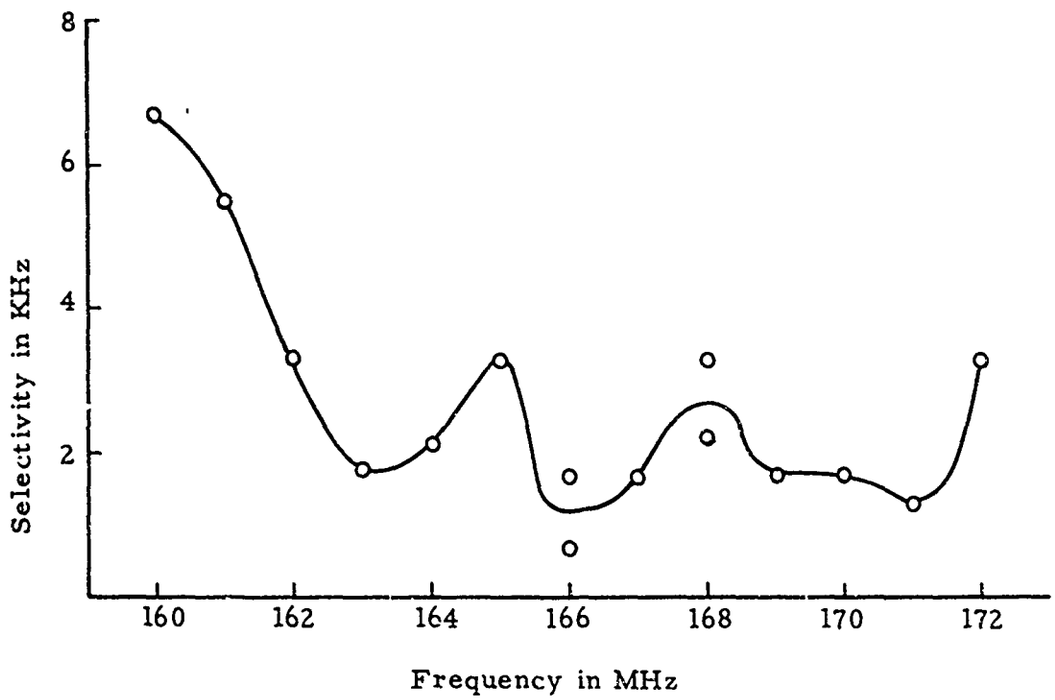

Figure 25 Selectivity of Cascaded Three-Sphere Circuit FSL

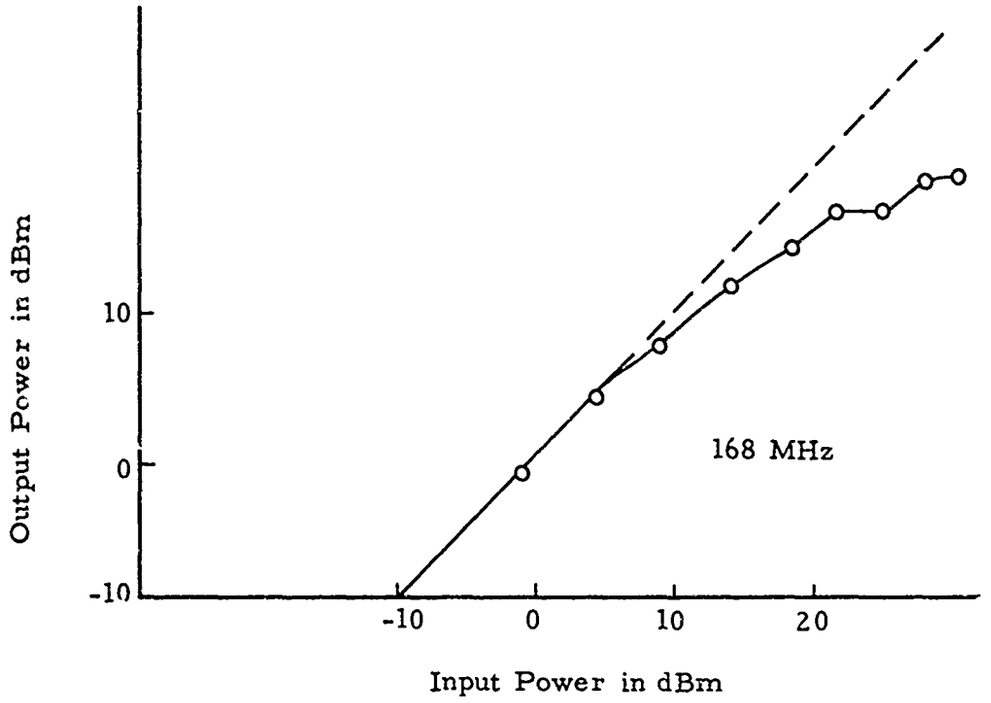

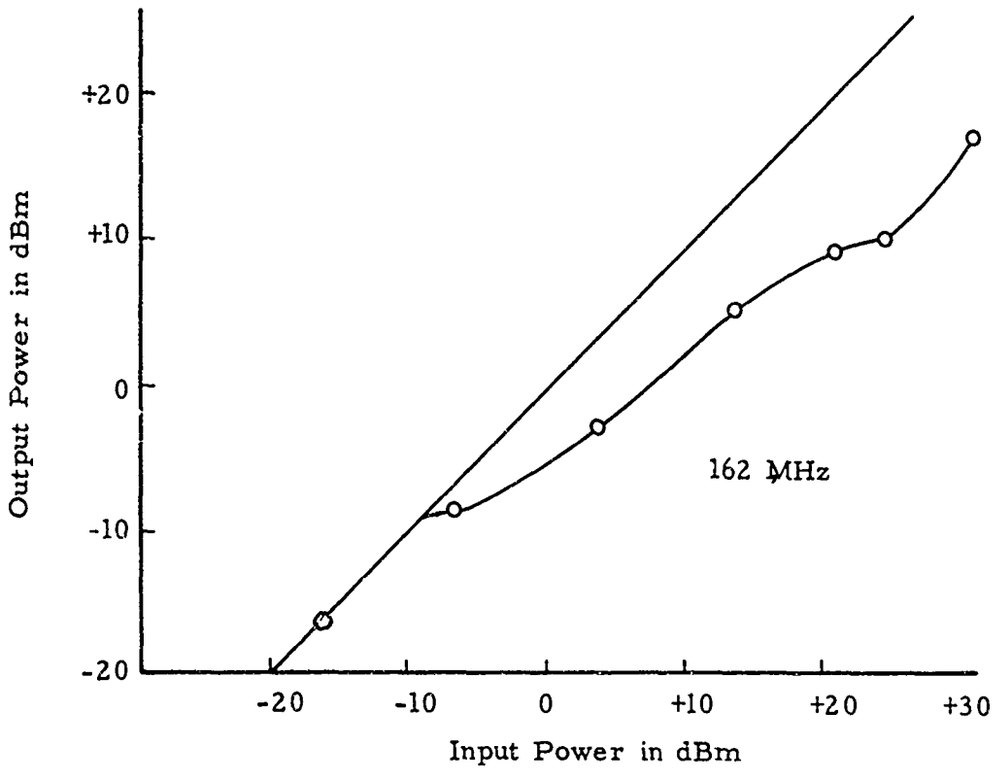

Figure 26 Limiting Curves for the Three-Sphere Cascaded-Parallel-Resonant-Circuit FSL Tuned to Cover the Band from 160.4 to 171.2 MHz

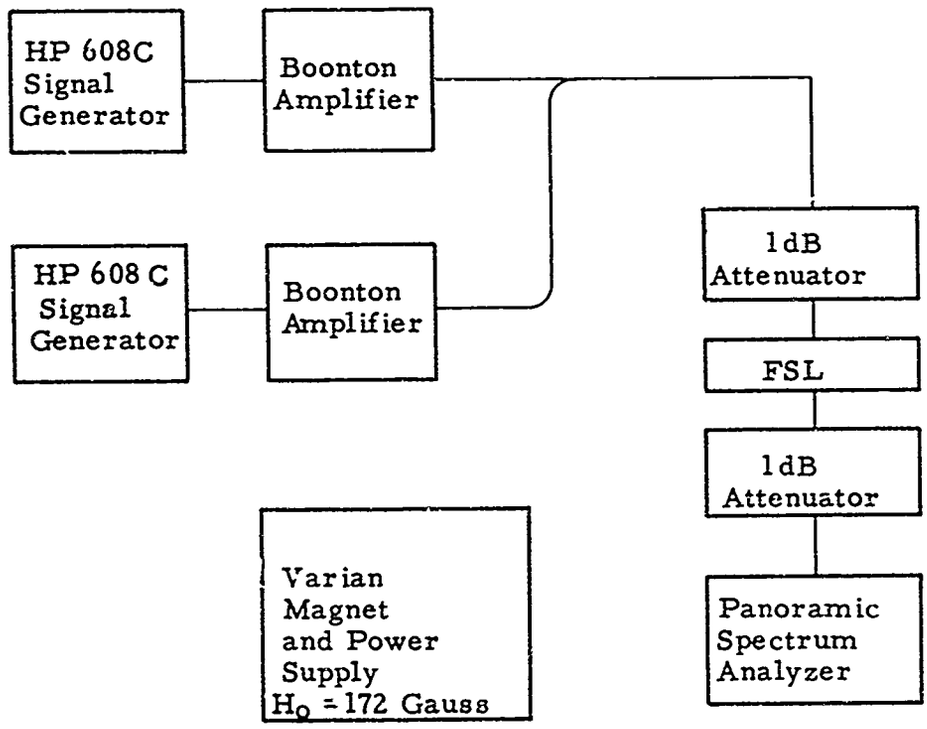

Figure 27 Block Diagram of System Used to Measure Intermodulation Characteristics

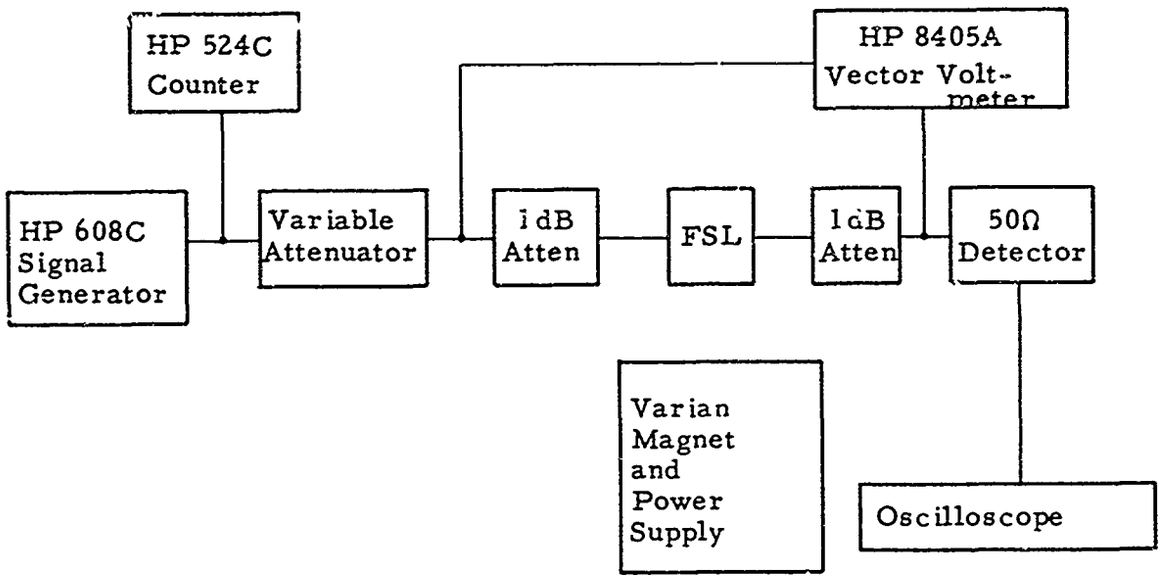

Figure 28 Block Diagram of System Used in Measuring Small Signal Amplitude and Phase Characeristics

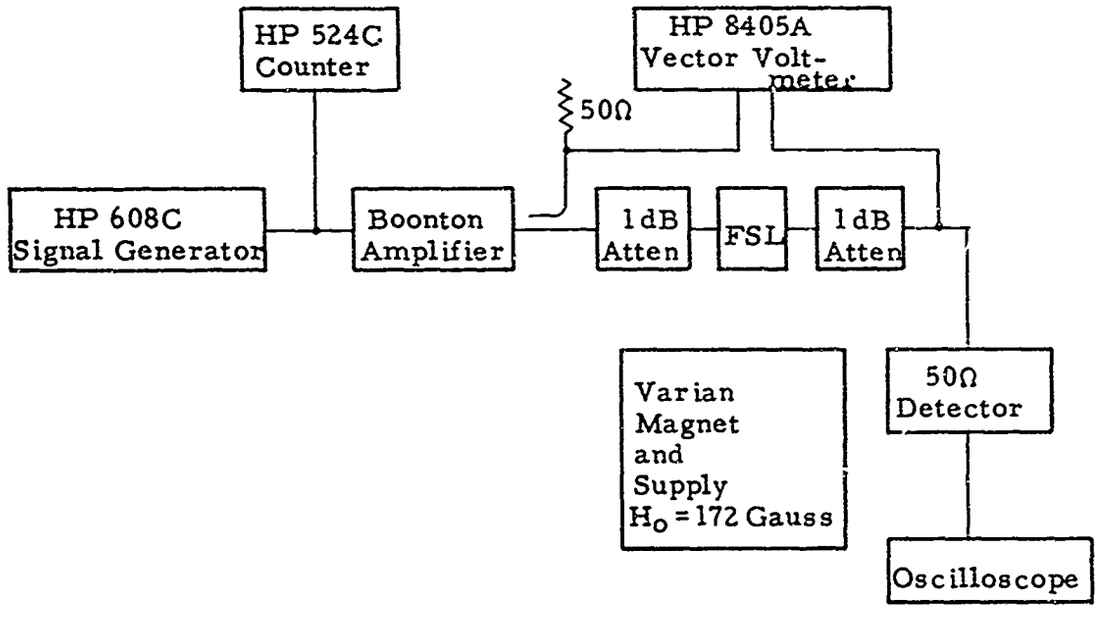

Figure 29 Block Diagram of System Used in Measuring Limiting Characteristics

VI.4.b Testing the Seven-Sphere Model

The seven-sphere circuit of Figure 7 was constructed and tested using the same heavily doped YIG:Ga spheres and the same test apparatus as shown in Figures 27-29. The final model is shown in Figure 30 complete with the test magnet (for size comparison). The test results are summarized in Figures 31 through 38. Note again the excellent intermodulation characteristics resulting from the selectivity of 3 KHz. The small signal response shows good out-of-band rejection as well as a linear phase response across the passband.

The seven-sphere FSL could be tuned to have good limiting (about 18 dB) over a very small region (about 1 MHz) in one part of the band by tuning while observing the transient response to a square wave input; however, such tuning degraded the insertion loss by 10 to 20 dB (to as high a loss as 35 dB) and would usually result in a non-uniform small signal passband response. By tuning for minimum insertion loss and a flat passband response, the limiting of 10-12 dB (as indicated in Figure 34) was achieved with 12 dB insertion loss. By tuning for an intermediate condition, the limiting of 14-15 dB of Figure 35 could be obtained across the entire band with an insertion loss of about 24 dB.

With the flat small signal response in the passband, the limiting curve of Figure 36 was obtained. Note the slight limiting found at low input power levels. This is due to exciting extremely low threshold modes (possibly those that don't couple tightly to the surface of the sphere). This small signal limiting was also noticed in most other limiting curve measurements and does not degrade the FSL performance to any significant extent.

In summary, note that both types of FSL's tested depicted frequency selective limiting and produced very little intermodulation between a large undesired interfering component and a small signal. With both FSL circuits, but particularly in the seven-sphere model, there is a large variation in threshold level across the band due to the different filtering effect of the circuitry prior to each sphere. This restricted the seven-sphere model to be no wider band than its first or perhaps first two circuit sections allowed. The high insertion loss of the seven-sphere circuit was a result of the tuning required to force the first few circuits to produce the most dynamic range (insertion loss had to be increased more than 10 dB above the minimum for the seven-sphere circuit). The approximately linear phase response was a result of the shape of the passband chosen.

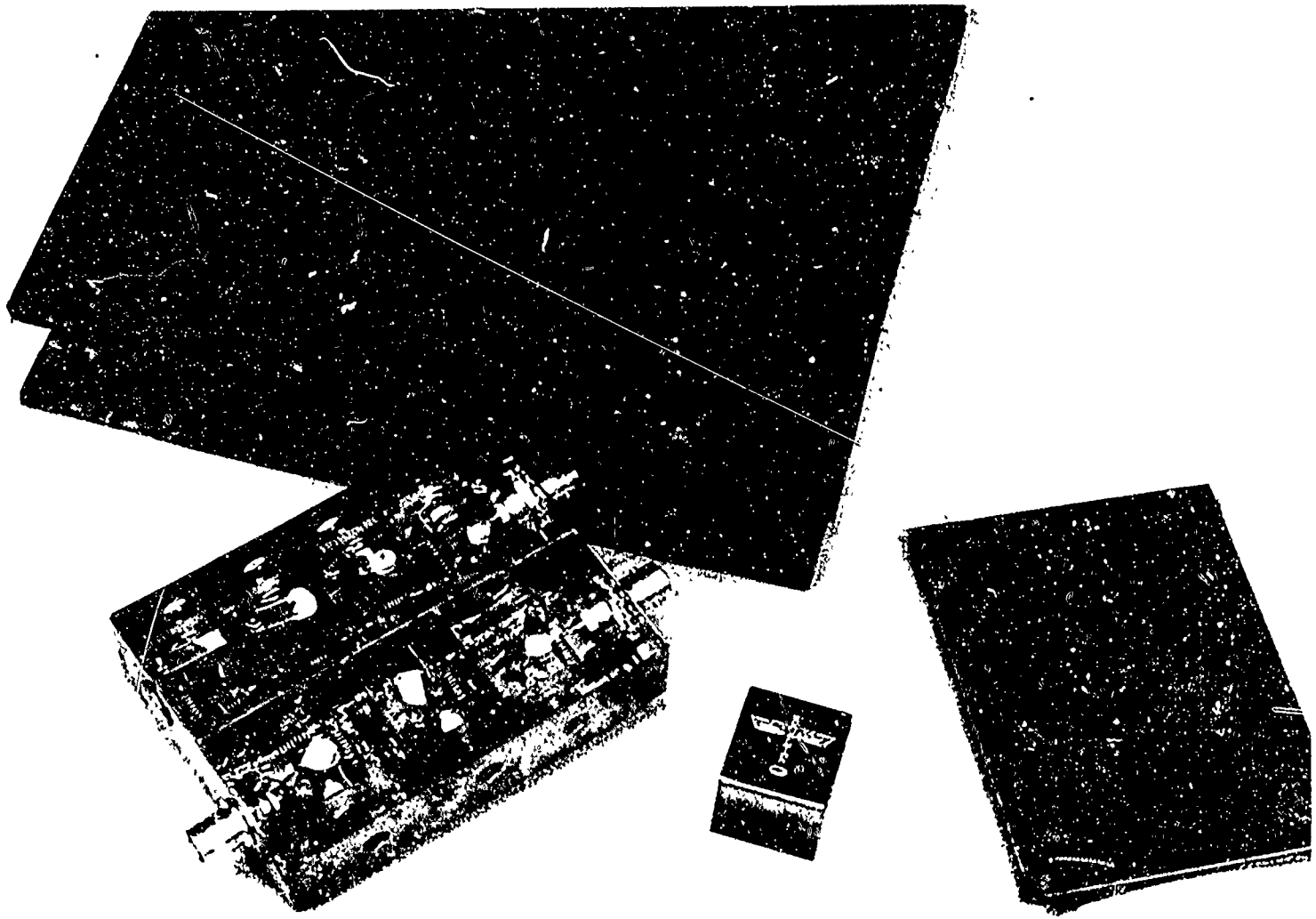

Figure 30 Picture of Seven-Sphere FSL

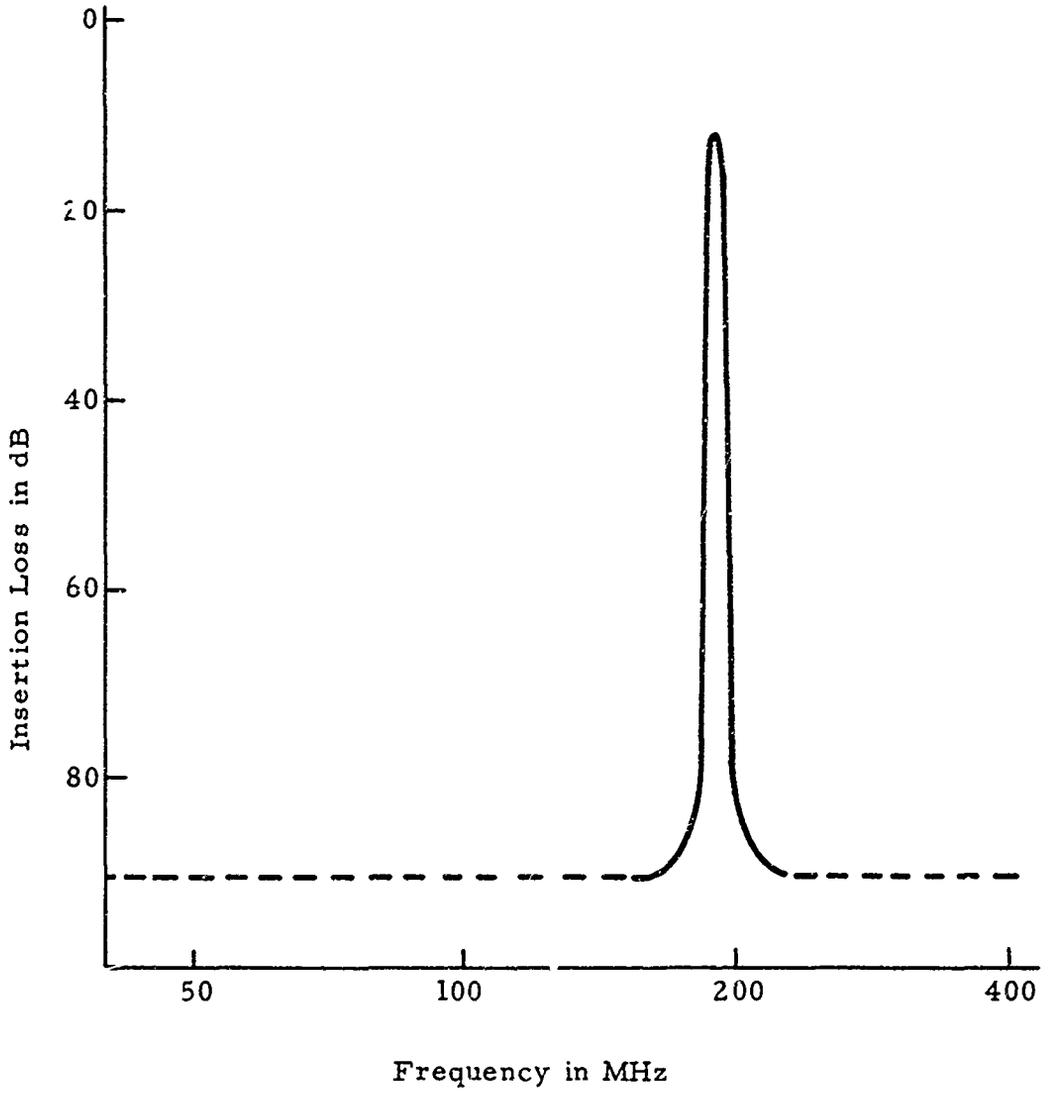

Figure 31 Measured Small Signal Response of Seven-Sphere Series-Resonant-Circuit FSL

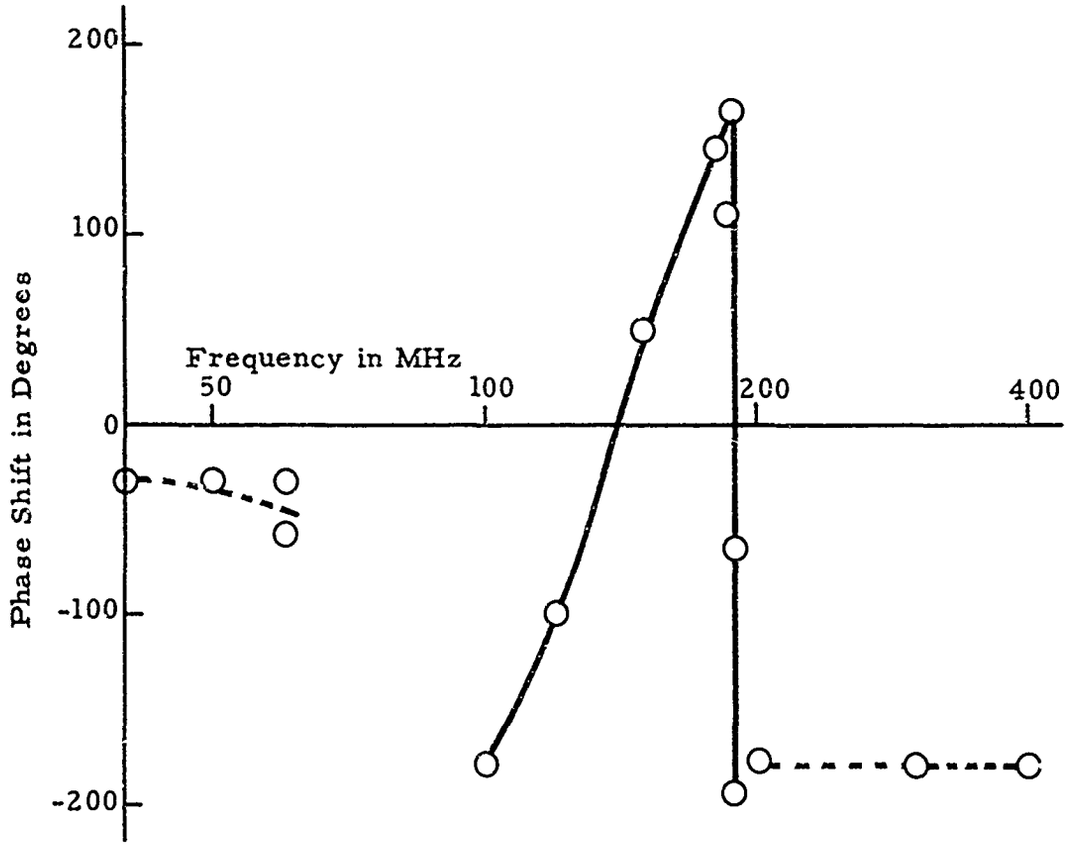

Figure 32 Phase Response of Seven-Sphere FSL

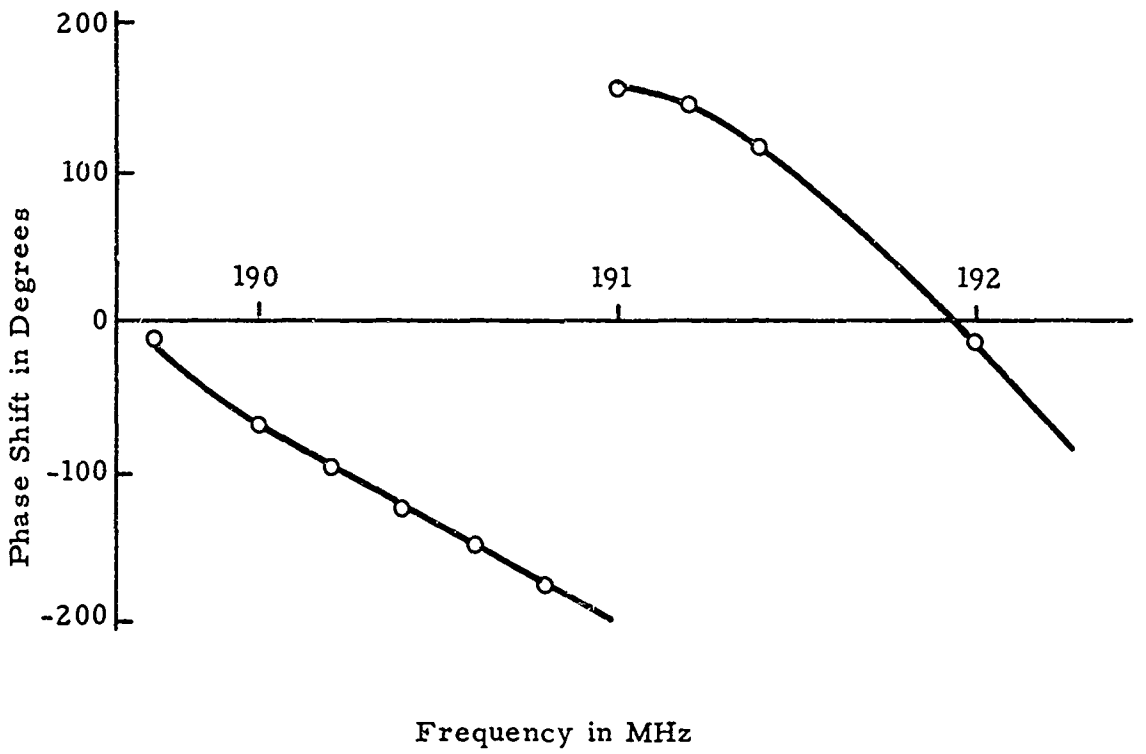

Figure 33 Phase Response of Seven-Sphere FSL

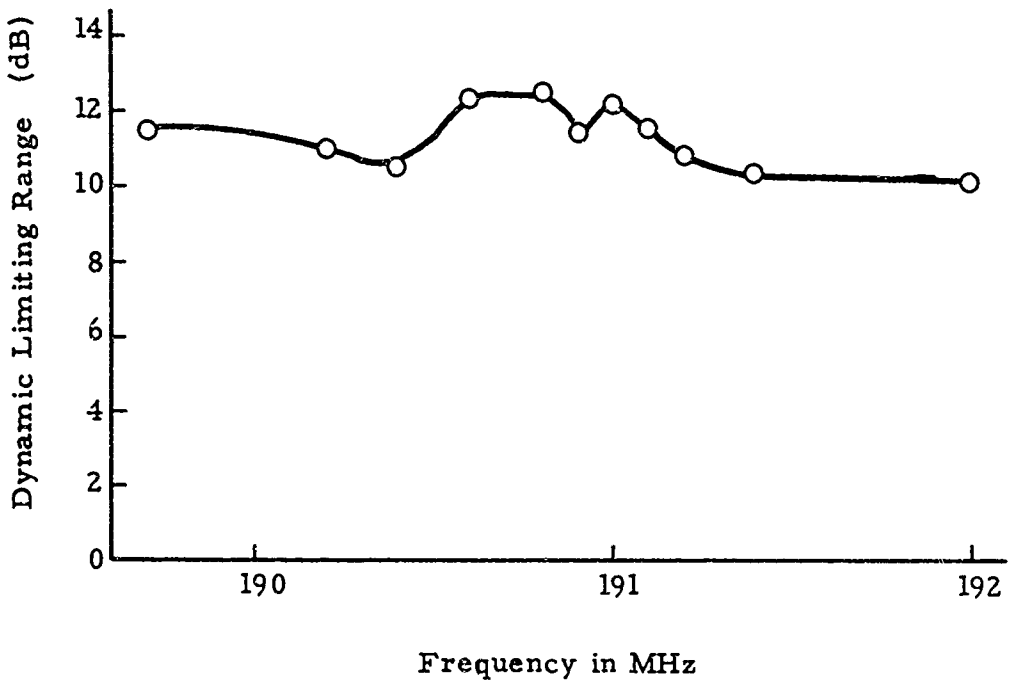

Figure 34 Dynamic Limiting Range of Seven-Sphere Series-Resonant-Circuit FSL

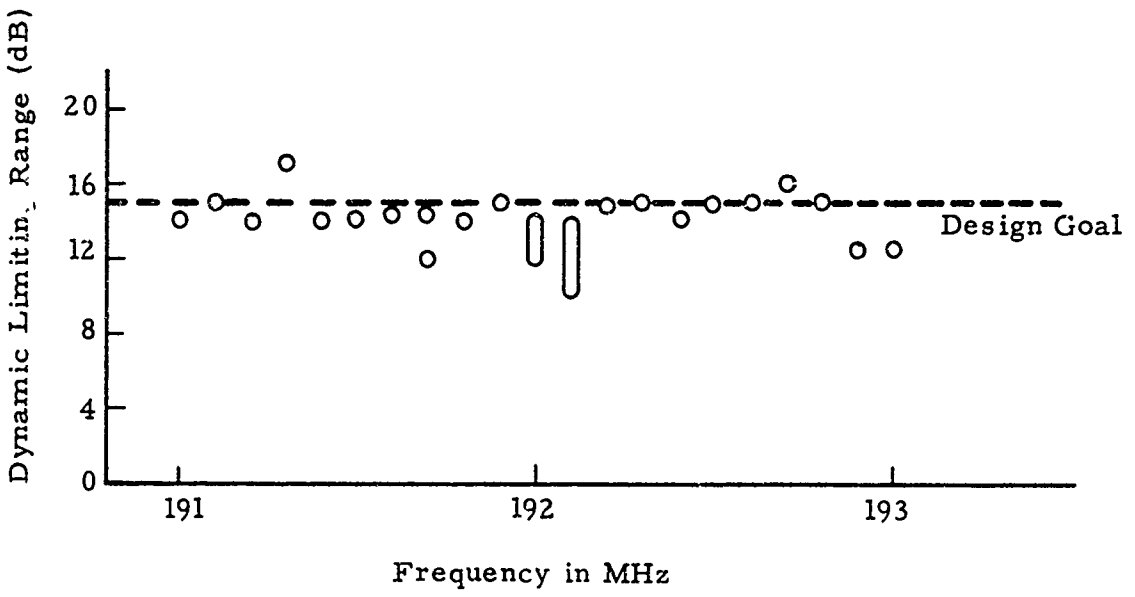

Figure 35 Dynamic Limiting Range for Seven-Sphere FSL When Adjusted for Good Limiting

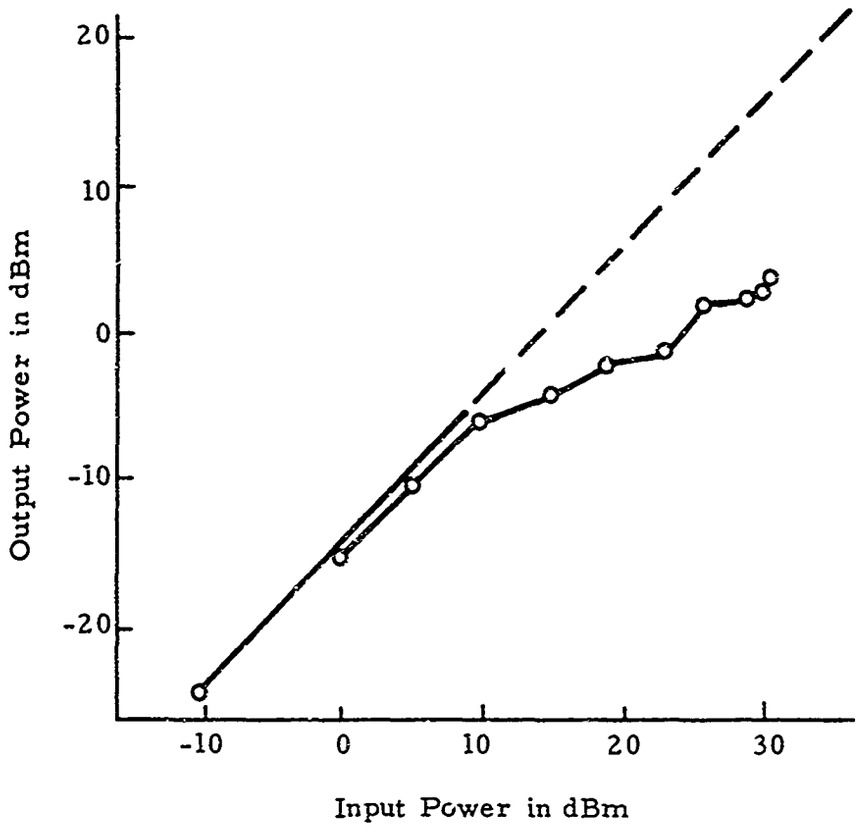

Figure 36 Limiting Curve for Seven-Sphere Cascaded-Series-Resonant-Circuit FSL

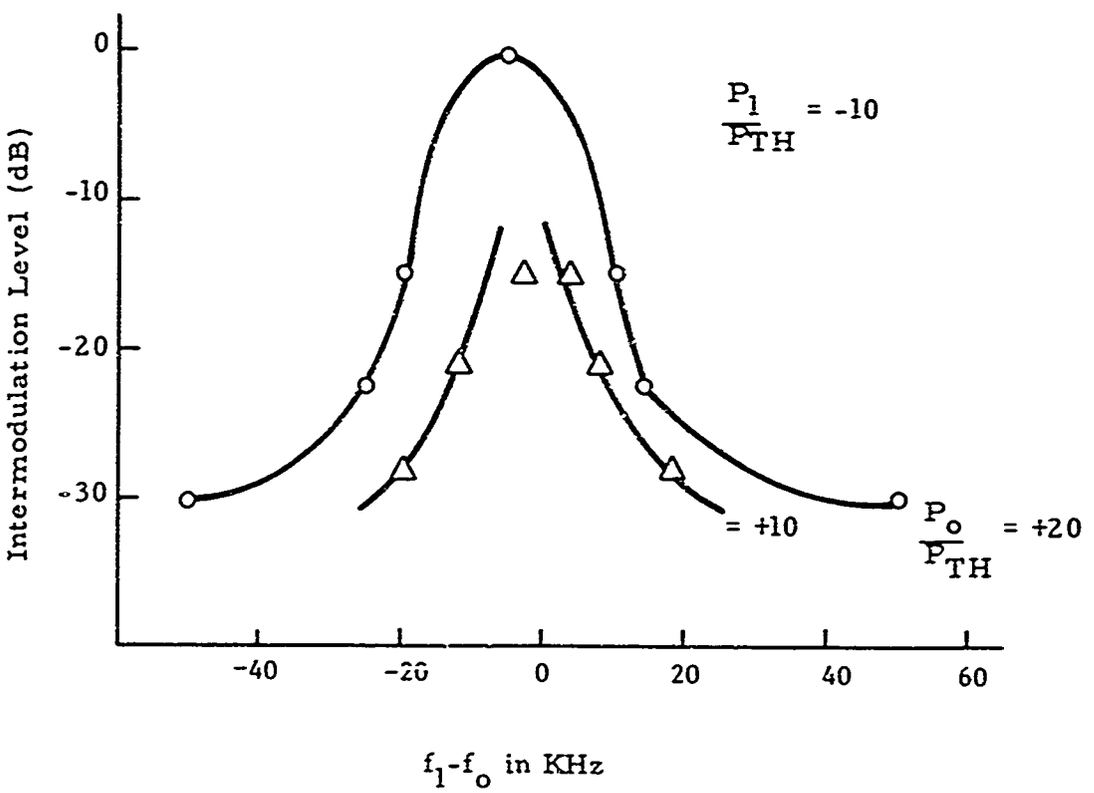

Figure 37 Level of Largest Intermodulation Component with Respect to the Suppressed Small Signal for a Seven-Sphere FSL

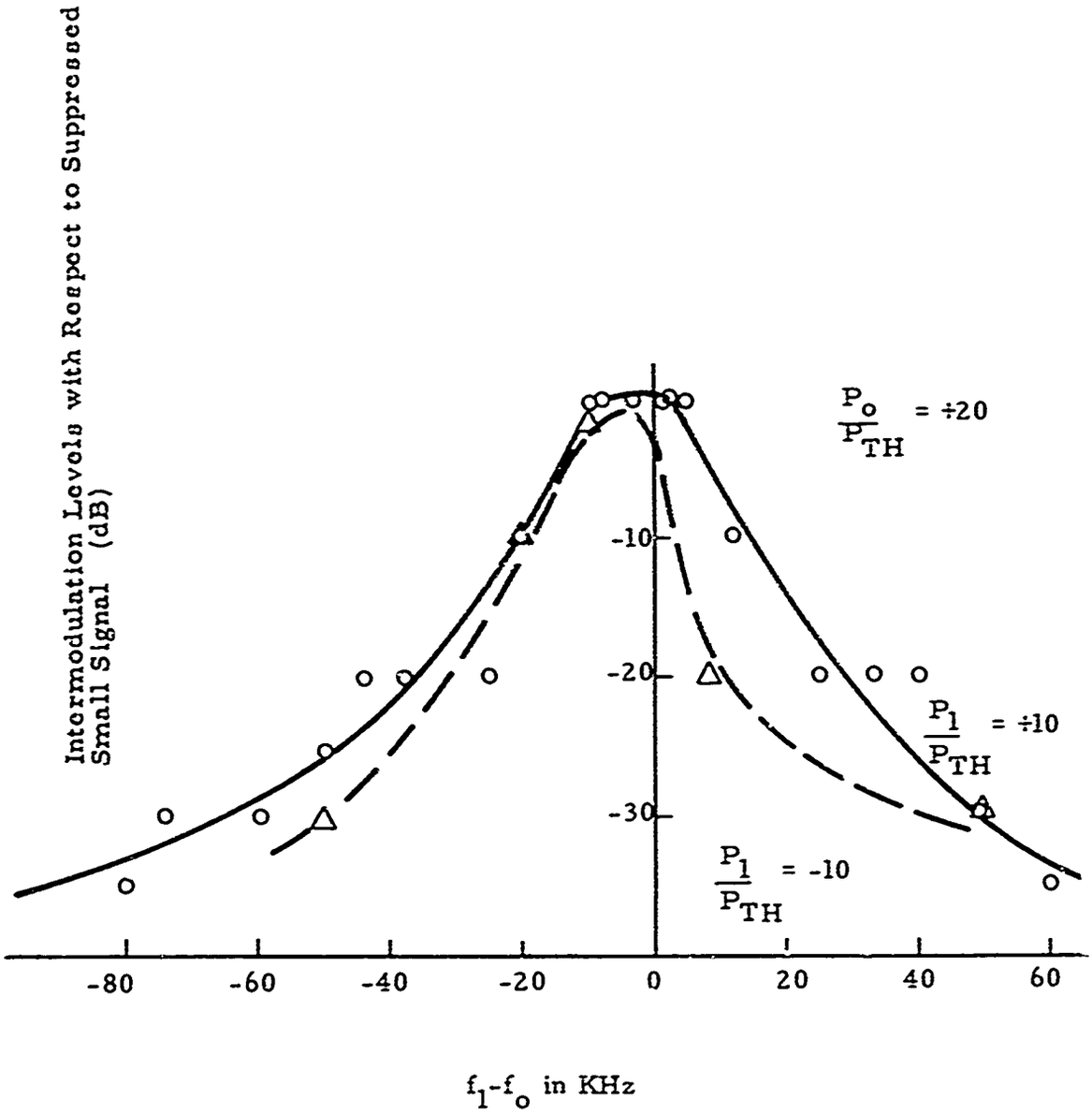

Figure 38 Intermodulation Levels Found Using the Seven-Sphere FSL with Different Small-Signal Levels

Either the amplitude or phase response could be tailored to meet the demands of a particular application, but both are related to each other by Hilbert transforms as with normal filter circuits.

SECTION VII

CONCLUSIONS

The basic goal of this contract was to determine whether a frequency selective limiter could be constructed for operation in the VHF band. The desired operating characteristics are those listed as design goals in Section I.

During the contract, extensive material tests were conducted, theories were presented and verified, and a final optimum material was chosen for use in a frequency selective limiter at VHF. This material is heavily doped single crystal polished YIG:Ga with saturation magnetization of 200 gauss. Circuits that used single spheres were evaluated in an effort to reduce the threshold, increase the bandwidth, and increase dynamic range. The conclusion reached was that the contract objectives could not be met with a circuit using only a single YIG:Ga sphere. Multiple sphere circuits were then designed and evaluated. The multiple sphere circuits came much closer to meeting the design goals. Compared to the single-sphere FSL's, the multiple-sphere models were found to have a higher dynamic range for a given bandwidth (or wider bandwidth for a given dynamic range), and were found to have less trouble with heating at high power levels (above 1/2 watt), but were found to have a higher insertion loss.

The comparison between the design objectives and the measured characteristics of the final breadboard models is presented in Table 2. Both of the models listed demonstrated continuous frequency-selective limiting across the band (as opposed to having good characteristic at only isolated points in the band as existed prior to the contract).

The selecitivity of 3 KHz is far better than could easily be constructed by any other means at VHF. The intermodulation characteristics, especially those of the three sphere model, are also very good.

The bandwidth, dynamic limiting range and insertion loss were less than expected because the coil design and material shape did not provide the desired fill factor, and because the cascaded circuits used were found to have the inherent problem of providing unequal feed loss to the individual resonant circuits. The Q of the resonant circuits was found to provide almost basic limitation on the threshold,bandwidth, and dynamic limiting range . That is, the spheres must be in high Q structure to experience strong time varying magnetic fields at low input power levels. This makes broadbanding of the device difficult.

	Design Objectives	7-Sphere Model	3-Sphere Model
Frequency	150-250 MHz	191 MHz	166 MHz
Bandwidth (-3 dB)	20% to 1 Octave	2 MHz (1%)	11 MHz (6.6%)
Limiting Dynamic Range	15 to 30 dB	10 to 12 dB (14 to 17 dB)	8 to 12 dB
Magnetoelastic Q	400 to 10^7	$> 6(10^4)$	$> 6(10^4)$
Average Insertion Loss	3 dB to 0.5 dB	12 dB (~ 26 dB)	18 dB
Passband Ripple	± 2 dB to ± 0.5 dB	± 0.5 dB	2 dB
Limiting Threshold Level	0 dBm to -20 dBm	+ 10 dBm	-3 to + 20 dBm

Table 2

Comparison of Design Objectives and Measured Characteristics of Final Models

Further work on circuit design should be directed toward the evaluation of circuits for maintaining high resonant fields in the individual spheres while maintaining broad bandwidth of the overall FSL circuit. The possibility of using different material in each resonant inductor to better effect a uniform threshold over a wide band should be considered.

Several possibilities exist for making substantial progress in improving the FSL operating characteristics. Although the threshold level cannot be lowered significantly by material choice, the power handling capability of the material could be increased by doping the material with a magnetic atom, as will be discussed in the next section.

In summary, good frequency selective action has been obtained across entire bandwidths of 1 to 11 MHz at VHF. Very little intermodulation was found between a large limited interference component and a small signal.

SECTION VIII

RECOMMENDED FOLLOW-ON PROGRAM

To make the most significant improvement in the operating characteristics of the VHF frequency-selective limiter, the dynamic limiting range and/or bandwidth should be increased. The following discussion briefly outlines a short program that would lead to such a goal.

The dynamic limiting range is restricted on the lower end by the threshold power level, and on the upper end by the internal crystal heating (nonlinear magnetoelastic effects). The threshold could possibly be reduced by placing the YIG:Ga spheres in a vacuum to reduce the surface losses. This may also increase the device mode density threby reducing the relaxation oscillations. The decoupling of the ferrimagnetic material from the air will also increase the elastic Q and make the FSL more selective.

The upper end of the dynamic limiting range can be extended by making the doped YIG a better heat conductor. This could be done by lightly doping the YIG:Ga with a magnetic atom like dysprosium to increase the spin-spin coupling. Although the resulting magnetic losses would be higher (higher spinwave threshold), the FSL does not operate with much coupling to the spinwaves, so that no degradation in selectivity should be encountered. Airtron (Division of Litton Industries, producing ferrimagnetic materials to order) claims that only about 0.001% doping with a magnetic atom will be enough to produce a noticeable change in the power handling capability. There is a high degree of confidence that magnetic-ion doping will increase the dynamic limiting range of the FSL.

To further increase the dynamic limiting range, encapsulation of the spheres in a helium atmosphere could be attempted. Tests already conducted during this contract using a helium atmosphere indicate that an increase of about 3 dB in the FSL dynamic limiting range is possible if the helium touches the YIG:Ga surface. This may be due to the good heat absorbing ability of the helium (without providing surface damping to the elastic modes). The use of helium to remove the heat would compliment any increase in thermal conductivity of the YIG which can be achieved as described in the previous paragraph.

The tests suggested above could be accomplished by procuring the magnetic-ion doped YIG:Ga and testing the FSL operation (using a single resonant circuit) using both a vacuum and a helium atmosphere surrounding the sphere. An increase of 10 dB in dynamic limiting range or a factor of 3 in bandwidth is expected.

In the area of circuit design, two prospects should be considered: 1) the broadband circuit design discussed in Section IV should be evaluated, and 2) some consideration should be given to increasing the fill factor by changing material shape or by redesign of the resonant structure. The modified Tchebycheff broadband filter should be evaluated for field strength in the resonant coils. Variations in the apparent threshold of a sphere in each of the inductors should be reduced by choosing a slightly different doping or orientation. Although this will produce a net increase in threshold, the magnetic-ion doping may offset this and a uniform dynamic range may be available across the wide passband.

An alternate follow-on program would be to construct an FSL that would operate at about 400 to 500 MHz. This device could have the same design goals as stated in Section I and would be more easily attained. At this higher frequency, transverse pumping could be used. The variation in threshold across a wide band expected for a transverse pumped FSL could be offset by the positioning of the resonant circuits. In addition, the use of distributed rather than lumped constant circuits could be considered. Such a device would be quite small and would have 4-5 times the mode density (for the same size spheres) as available using the 0.1" diameter spheres at VHF.

In summary, the following tests will provide a large increase in dynamic limiting range and bandwidth of the VHF FSL.

1) Determine the effect of using magnetic-ion doped YIG on the dynamic limiting range.

2) Operate an FSL with the YIG spheres a) in a vacuum and b) in a helium atmosphere to determine the effect on threshold and dynamic limiting range.

3) Consider other circuit designs to improve the fill factor and to widen the bandwidth.

4) Determine whether a major improvement would result by relaxing the frequency requirement for the FSL to operate at 300-500 MHz. The improvement sought should be mainly in circuit design (improving the fill factor and dynamic range) since improvements in mode density and reduction in relaxation oscillation are expected.

REFERENCES

1. Technical Proposal, "Wideband Magnetoelastic Frequency Selective Limiter for VHF," Boeing Internal Document Number D2-125343-1, 1967.

2. R. W. Orth, "Frequency-Selective Limiters and their Applications," IEEE G-EMC Special Filtering Issue, June 1968.

3. R. W. Orth and D. R. Jackson, "Wideband Magnetoelastic Frequency Selective Limiter for VHF," Boeing Internal Document Number D2-125920-1, July 1968. (First Technical Report on Contract F30602-68-C-0072.)

4. E. Schloman and R. I. Joseph, "Parametric Excitation of Phonons in Magnetic Materials by Means of Parallel Pumping," Raytheon Technical Memorandum T-800, October 8, 1968.

5. R. L. Comstock, "Parallel Pumping of Magnetoelastic Waves in Ferromagnets," Journal of Applied Physics, Vol. 35, p. 2427, August 1964.

6. A. Giarola and G. Fitzsimmons, "Spin Wave Frequency-Selective Limiters," Boeing Internal Document Number D2-125322-1, May 1967.

7. Boeing Internal Memo ET-67-21 by Barry Woo to J. M. Bartlemay, August 15, 1968, Subject "LC Bandpass Filters with Equal Inductances."

8. Guillemin, Introductory Circuit Theory MIT, 1953.

UNCLASSIFIED

Security Classification

DOCUMENT CONTROL DATA - R & D

(Security classification of title, body of abstract and indexing annotation must be entered when the overall report is classified)

1. ORIGINATING ACTIVITY (Corporate author) The Boeing Company Seattle, Washington 98124	2a. REPORT SECURITY CLASSIFICATION UNCLASSIFIED 2b. GROUP NA

3. REPORT TITLE

WIDEBAND MAGNETOELASTIC FREQUENCY SELECTIVE LIMITER FOR VHF

4. DESCRIPTIVE NOTES (Type of report and inclusive dates)

Final Report 1 January 1968 to 31 December 1968

5. AUTHOR(S) (First name, middle initial, last name)

Roger W. Orth

6. REPORT DATE February 1969	7a. TOTAL NO. OF PAGES 67	7b. NO. OF REFS 8
8a. CONTRACT OR GRANT NO. F30602-68-C-0072 b. PROJECT NO. 5573 c. Task No. d. 557301	9a. ORIGINATOR'S REPORT NUMBER(S) D2-125920-2 9b. OTHER REPORT NO(S) (Any other numbers that may be assigned this report) RADC-TR-69-21	

10. DISTRIBUTION STATEMENT

This document is subject to special export controls and each transmittal to foreign governments, foreign nationals or representatives thereto may be made only with prior approval of RADC (EMIAD), GAFB, N.Y. 13440.

11. SUPPLEMENTARY NOTES RADC Project Engineer Henry Friedman AC 315 330-3591	12. SPONSORING MILITARY ACTIVITY Rome Air Development Center (EMIAD) Griffiss Air Force Base, New York 13440

13. ABSTRACT

In this Second Technical Report, the results of one year's progress are summarized for RADC Contract F30602-68-C-0072, titled "Wideband Magnetoelastic Frequency-Selective Limiter for VHF Band," for the construction of a frequency-selective Limiter that uses parametric generation of subharmonic magnetoelastic modes in ferrimagnetic materials. Special attention is given to the results of tests performed during the second six months on the broadband models constructed. Based on the theory of operation and test results presented in the First Technical Report, the philosophy of broadband frequency-selective limiter circuit design is presented. The importance of pumping direction, material selection, and orientation is discussed.

The material used in the final model is YIG:Ga, a highly doped garnet. The final orientation was made to provide a low internal saturation magnetic field to provide a low limiting threshold. Tests of the final model indicated that extremely selective limiting (about 3 KHz selectivity), low intermodulation levels, and linear small signal phase response are obtainable at VHF.

DD FORM 1 NOV 65 1473

UNCLASSIFIED

Security Classification

UNCLASSIFIED

Security Classification

14 KEY WORDS	LINK A		LINK B		LINK C	
	ROLE	WT	ROLE	WT	ROLE	WT
Limiters						
Bandpass Filters						
Tuned Circuits						
Coupling Circuits						

UNCLASSIFIED

Security Classification